Provided for non-commercial research and education use.
Not for reproduction, distribution or commercial use.

(This is a sample cover image for this issue. The actual cover is not yet available at this time.)

This article appeared in a journal published by Elsevier. The attached copy is furnished to the author for internal non-commercial research and education use, including for instruction at the authors institution and sharing with colleagues.

Other uses, including reproduction and distribution, or selling or licensing copies, or posting to personal, institutional or third party websites are prohibited.

In most cases authors are permitted to post their version of the article (e.g. in Word or Tex form) to their personal website or institutional repository. Authors requiring further information regarding Elsevier's archiving and manuscript policies are encouraged to visit:

http://www.elsevier.com/copyright

Author's personal copy

Aeolian Research 5 (2012) 21–42

Contents lists available at SciVerse ScienceDirect

Aeolian Research

journal homepage: www.elsevier.com/locate/aeolia

Review Article

Impacts on iron solubility in the mineral dust by processes in the source region and the atmosphere: A review

Zongbo Shi [a,*], Michael D. Krom [b], Timothy D. Jickells [c], Steeve Bonneville [d], Kenneth S. Carslaw [b], Nikos Mihalopoulos [e], Alex R. Baker [d], Liane G. Benning [b]

[a] School of Geography Earth and Environmental Sciences, University of Birmingham, Birmingham, UK
[b] School of Earth and Environment, University of Leeds, Leeds, UK
[c] School of Environmental Sciences, University of East Anglia, Norwich, UK
[d] Earth System Modelling Department, Earth & Environmental Sciences, Université Libre de Bruxelles, Bruxelles, Belgium
[e] Environmental Chemical Processes Laboratory, University of Crete, Heraklion, Greece

ARTICLE INFO

Article history:
Received 17 August 2011
Revised 6 March 2012
Accepted 6 March 2012

Keywords:
Solubility
Chemical weathering
Acid processing
Cloud processing
Gravitational settling

ABSTRACT

Mineral dust is a complex entity containing a range of iron minerals including poorly crystalline to crystalline iron oxides to clay minerals. Important progress has been made to characterize iron mineralogical compositions in the dust recently. These include the quantification of the content of crystalline hematite and goethite, which appear to show a regional variation in North Africa as a result of the differences in the degree of chemical weathering. Fractional Fe solubility (dissolved to total iron, FFS) in the atmospheric aerosols has been reported to range from 0.1% to 80%. However, FFS is usually less than 0.5% in the non-atmospherically-processed dust, suggesting that FFS can be enhanced by atmospheric processes. One of the atmospheric processes, gravitational settling of dust, which has been previously hypothesized to cause the abovementioned enhancement of FFS during dust transport has been shown to be insignificant. Cycling of dust particles in the clouds, in which pH is usually higher than 4, and in the aerosol phase, in which pH is usually substantially lower, can significantly affect iron speciation and FFS. Laboratory experiments showed that a significant amount of iron (>0.5%) can only be solubilized in the dust when pH is lower than 4. These laboratory data suggest that acid processing rather than cloud processing might be a prime mechanism to cause an increase in FFS in the dust during transport. Further laboratory studies, field measurements, and modelling are needed to increase the ability of models to quantify the atmospheric processing of iron in the dust.

© 2012 Elsevier B.V. All rights reserved.

Contents

* Corresponding author.
E-mail address: z.shi@bham.ac.uk (Z. Shi).

1875-9637/$ - see front matter © 2012 Elsevier B.V. All rights reserved.
http://dx.doi.org/10.1016/j.aeolia.2012.03.001

Author's personal copy

1. Introduction

In late 1980s, at an informal lecture at the Woods Hole Oceanographic Institution, oceanographer John Martin said, "*Give me a half tanker of Fe, and I will give you an ice age.*" These provocative words were related to a theory subsequently known as the "Fe hypothesis", which was proposed by Martin and Fitzwater (1988) and Martin (1990), based on the inverse relationship of particulate Fe supply and measured CO_2 concentration in the Vostok ice core (Martin, 1990). The first meso-scale Fe fertilization experiment in 1993 confirmed that Fe limitation can control rates of phytoplankton productivity and biomass in the Southern Ocean. Up to 2007, 11 additional meso-scale Fe fertilization experiments have been carried out in various so-called HNLC (high nutrient low chlorophyll) areas. These experiments have unequivocally shown that Fe supply limits production in one-third of the world ocean, where surface macronutrient concentrations are perennially high (de Baar et al., 2005; Boyd et al., 2007) and atmospheric aerosol (dust) inputs are low (Jickells et al., 2005). The findings of these Fe enrichment experiments showed that the Fe supply controls the dynamics of plankton blooms, which in turn affects the biogeochemical cycles of carbon and ultimately influences the Earth's climate system (de Baar et al., 2005; Boyd et al., 2007). Furthermore, there is evidence of the impact of changes in Fe supply on atmospheric CO_2 during glacial cycles provided by ice cores (Martin et al., 1989; Petit et al., 1999; Lambert et al., 2008; Sigman and Boyle, 2000; Watson et al., 2000; Ridgwell and Watson, 2002; Röthlisberger et al., 2004).

While it has been recognized that Fe supplied by atmospheric aerosol is globally a rather small fraction of the total Fe inputs to the oceans, it is disproportionately important in open ocean waters because other sources of Fe (Jickells et al., 2005), such as the impact of riverine and resuspension is introduced at the ocean margins and trapped near the coast (Poulton and Raiswell, 2002; Croot and Hunter, 1998; Elrod et al., 2004; Raiswell and Canfield, 2012). Globally, mineral dust is the dominant source of Fe in atmospheric aerosol inputs to the open ocean. Mineral dust is mainly produced in the desert regions of the world. Dust originates from soils in the desert which are physically separated and uplifted to the atmosphere. Most of the Fe delivered from mineral dust to the surface ocean is highly refractory and only some of the atmospheric Fe is bioavailable (Achilles et al., 2003; Rubin et al., 2011; Visser et al., 2003). The bioavailable Fe fraction of atmospheric dust has been suggested to regulate and, at times, limit the primary productivity in large areas of the open oceans. Even in regions where phytoplankton growth is not Fe limited, such as the subtropical North Atlantic, dust input may affect primary productivity by stimulating nitrogen fixation (Mahaffey et al., 2003; Mills et al., 2004; Moore et al., 2009). As a result, the supply of bioavailable Fe from mineral dust can influence the CO_2 uptake from the atmosphere and affect Earth's climate (Jickells et al., 2005; Shao et al., 2011). Such impact on the climate could in turn affect the dust emission and transport (Shao et al., 2011; Jickells et al., 2005).

One of the major uncertainties of the interplay between the Fe biogeochemical cycle and phytoplankton biodynamics is the flux of labile/bioavailable Fe delivered via atmospheric dust to the ocean surface (Jickells et al., 2005; Mahowald et al., 2005, 2009; Breitbarth et al., 2010; Ridgwell and Watson, 2002). Since the Fe bioavailability cannot be directly measured chemically, it is often assumed that the dissolved Fe or highly reactive Fe in the dust is bioavailable (e.g., Fan et al., 2006; Raiswell et al., 2008). We realized that dissolved Fe and highly reactive Fe may contain nanoparticles, which are not completely bioavailable (e.g., Chen and Siefert, 2003; Visser et al., 2003). However, there is no better proxy at the present, thus in the following we mainly discuss dissolved Fe. The flux of the dissolved Fe can be calculated as

$$\text{Flux}_{\text{dissolved Fe}} = \text{Deposition Flux}_{\text{dust}} \times \text{FeT} \times \text{Fractional Fe solubility} \quad (1)$$

in which FeT is the total Fe content in the dust and the fractional Fe solubility (FFS) is the percentage of dissolved to FeT. The estimated total flux of dust to the ocean is less uncertain (Jickells et al., 2005; Mahowald et al., 2005; Jickells and Spokes, 2001), except in the most remote Southern Ocean (Wagener et al., 2008a; Boyd et al., 2004). FeT in the dust is also less uncertain and is usually from 1% to 5% in dust from different source regions (e.g., Guieu et al., 2002; Hand et al., 2004; Mahowald et al., 2005). In most atmospheric models, FeT is assumed to be 3.5% (Hand et al., 2004; Luo et al., 2005; Meskhidze et al., 2005; Fan et al., 2006; Solmon et al., 2009; Ito and Feng, 2010). However, the FFS term varies considerably from ~0.1% to more than 80%, with higher solubility values generally observed when dust mass concentrations are low both over remote parts of the oceans and over polluted areas (e.g., Hand et al., 2004; Chen and Siefert, 2004; Baker and Jickells, 2006; Sedwick et al., 2007; Mahowald et al., 2005; Kumar and Sarin, 2010; Erel et al., 1993; Sedlak et al., 1997; Theodosi et al., 2010).

The FFS in the dust (before being deposited to the ocean) is controlled primarily by (i) the mineralogy of the soils in the source area and (ii) atmospheric processes that can convert low-reactivity Fe-bearing minerals into highly soluble/bioavailable forms of Fe (nanoparticle for instance). There are a number of processes occurring once the dust is dry deposited to the ocean, which affect the dissolved Fe supply to the ocean. Such processes were discussed in Baker and Croot (2010). We will focus on the processes before the dust being deposited to the ocean.

The key question to quantify the FFS is to understand the influence of environmental processes that control both the quantity and the quality of the Fe delivered to oceans via dust deposition.

Author's personal copy

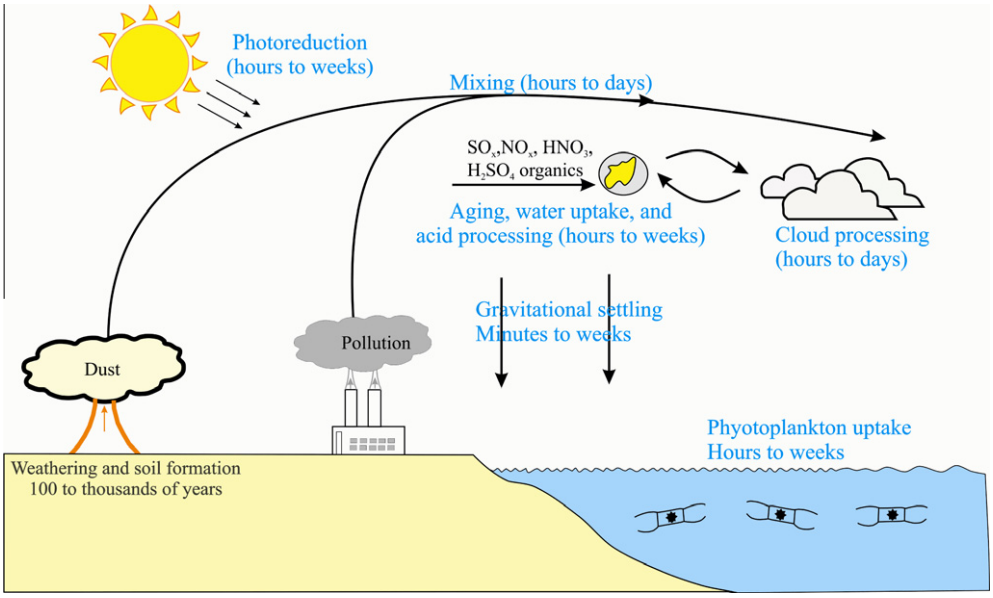

Fig. 1. A schematic diagram showing some of the most important processes controlling the speciation of Fe in the atmosphere and its subsequent deposition back to the land and/or ocean. Processes in the source regions include weathering and aging of Fe oxides, which affect the Fe mineralogy of dust, resulting in dust of different potential solubilities (Shi et al., 2011b). During transport, dust may mix with soot particles from biomass burning and other anthropogenic aerosols (e.g., Arimoto et al., 2006; Chuang et al., 2005; Kandler et al., 2007; Mackie et al., 2005, 2008; Luo et al., 2008; McConnell et al., 2008; Haywood et al., 2008; Hand et al., 2010). This mixture of particles may also take up sulphate, nitrate and organic ligands (e.g., Clarke et al., 2004; Zhang and Iwasaka, 1999; Zhang et al., 2003, 2006; Sullivan et al., 2007; Sullivan and Prather, 2007; Shi et al., 2008; Dall'Osto et al., 2010). During long range transport, dust undergoes gravitational settling, cloud processing, photo-reduction, and acid uptake/processing (Seinfeld and Pandis, 2006; Wurzler et al., 2000; Rosenfeld et al., 2001; Matsuki et al., 2010; DeMott et al., 2003; Sullivan et al., 2007; Dall'Osto et al., 2010). Cycles between dust, particularly aged dust (serving as cloud condensation nuclei, CCN) and clouds through condensation/evaporation processes can occur 5–10 times before the dust is deposited to the ocean (Seinfeld and Pandis, 2006).

The physical, chemical, and optical properties of mineral dust have been reviewed in Formenti et al. (2011) and Redmond et al. (2010). We summarized in this review what is known about the amount, the form and the mineralogy of Fe in the dust. We compiled here the present knowledge of how chemical weathering in the source area can control the amount and nature of Fe oxides and clays which are the major precursors of chemically reactive and hence bioavailable Fe in mineral dust. Once the dust is uplifted into the air another series of processes occur (Fig. 1) that change the mineralogy and speciation of Fe. A more detailed description is shown in Section 4.3. An important aspect of current research is to integrate observations and datasets into process-based quantitative relationships which can be incorporated into large-scale models to improve the quality of their predictions. Therefore, we finish this review by briefly summarizing the current work to simulate the atmospheric processing of Fe in the dust using mathematical models.

We would like to emphasize that, in addition to mineral aerosols originating from desert regions, biomass burning and anthropogenic pollution also provide Fe-bearing particles which can be a dominant source of bioavailable Fe in some areas of the ocean, particularly at places close to the East Asian continent in the North Pacific (Luo et al., 2008; Mahowald et al., 2009) and the North American (Sedwick et al., 2007; Sholkovitz et al., 2009). However in this review we concentrate on the atmospheric processing of mineral dust from desert regions and only mention these other forms of aerosols where they are necessary to understand field measurements and other observational data.

1.1. Definition and measurement of Fe solubility

Similar to the concerns in Baker and Croot (2010), we note the important difference in the definition of "solubility" between the atmospheric and geochemical communities. In the geochemical literature, the solubility of a specific mineral in a specific solvent and at particular conditions (e.g., pH, temperature, pressure) is the concentration (in fact, the activity) of a solute measured *in equilibrium* with a mineral phase and is therefore independent of mineral mass in the system considered. In that sense, the solubility of a given mineral is an exact thermodynamic parameter. We will use "solubility" to refer to that in a geochemical context. The solubility of Fe oxides are widely reported (reviewed in Cornell and Schwertmann, 2003) but that in the dust is not reported.

In the atmospheric literature, "solubility" of a sample is an operationally-defined ratio (as a percentage) of the dissolved Fe concentration (typically after filtration and passing through 0.2 or 0.45 μm pore size filter) in the filtrate relative to the total Fe contained in the bulk sample. This "solubility" is termed here as the "fractional Fe solubility (FFS)", which will be followed in this review. There is no direct relationship between the geochemical thermodynamic solubility and the atmospheric FFS for a dust sample. The FFS is sometimes measured during the transient stage (before thermodynamic equilibrium) at a particular point where mineral dissolution kinetics controls the concentration in solution. Therefore, FFS is heavily dependent on the properties of the sample and the following parameters:

The first is the extractant/solvent used. A number of extractants have been used to quantify the FFS for slightly different purposes. The simplest extractant is MilliQ (18.2Ω) water (e.g., Chen et al., 2006; Paris et al., 2010, 2011) which has a similar pH to that of the non-acidified cloud water. However the problem with MilliQ water is that it has a very limited buffer capacity and thus the pH will change depending on the particular dust sample being tested (e.g., Paris et al., 2011). It is thus paradoxically rather difficult to compare the results obtained, unless large amounts of water were used to avoid the change in pH and the precipitation of dissolved Fe. To overcome this problem a number of studies have used weak buffers such as ammonium acetate, pH = 4.7 (e.g., Sarthou et al., 2003; Baker et al., 2006a,b, 2007), or formate-acetate buffer at pH 4.5 (Chen and Siefert, 2003, 2004). These extractants allow

Author's personal copy

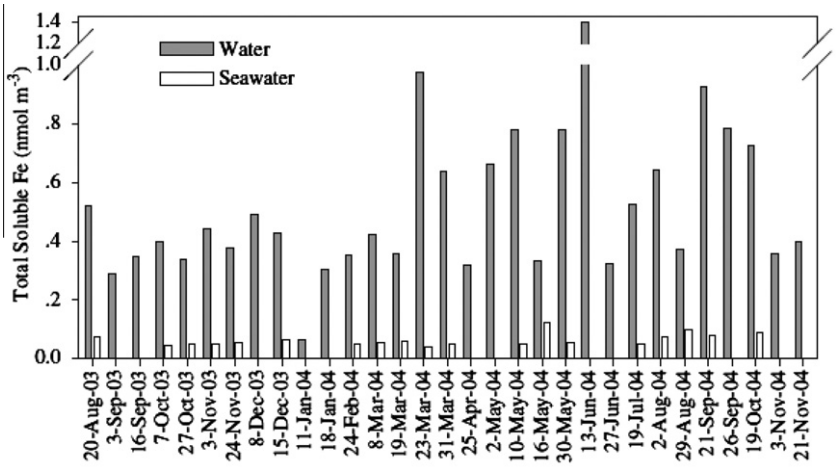

Fig. 2. Concentrations of total dissolved Fe (nmol m^{-3}) extracted by pure water (dark bars, $n = 31$) and Sargasso seawater (white bars, $n = 19$) from aerosol samples collected in the Gulf of Aqaba. Reproduced from Chen et al. (2006) by permission of Elsevier.

the results between different mineral aerosols to be compared more easily. Seawater has also been used as an extractant. Seawater has a sufficiently large pH buffer capacity (e.g., Chen et al., 2006, 2008; Bonnet and Guieu, 2004). However, at pH ~8.2, Fe solubility is at its lowest, reaching usually sub-nM concentration in synthetic sea water (Liu and Millero, 1999, 2002), although it is typically in the 1–2 nM range in open ocean seawater (Kuma et al., 1998a; Schlosser and Croot, 2008) and higher yet in coastal waters (Kuma et al., 1998b; Schlosser and Croot, 2009). While studies have been carried out which compare FFS of the same aerosol sample in MilliQ water to that in seawater, it is always higher in MilliQ water (Buck et al., 2006, 2010a; Chen et al., 2006, see Fig. 2), which is not surprising because of the higher pH in seawater. Bonnet and Guieu (2004) also showed that the FFS in the seawater is dependent on the amount of dust (e.g., grams) added to a certain volume of seawater. Thus although carrying out dissolution experiments in seawater is clearly relevant for the actual input of Fe from atmospheric dust into the surface ocean, it is not very useful for studying the nature and effect of atmospheric processes on mineral dust. Also, as Baker and Croot (2010) pointed out, the nature (e.g., origin, pH, organic ligand concentration) of the seawater used in the experiment will also have a strong influence on the Fe solubility obtained. Finally several studies have determined the solubility of Fe in pH 2 solution (Trapp et al., 2010; Journet et al., 2008; Shi et al., 2011b). Such studies are useful for determining the potential solubility of Fe during atmospheric processing since thermodynamic modelling suggested that a pH of 2 or lower is often expected in the aerosol water (Zhu et al., 1992; Meskhidze et al., 2003; Nenes et al., 2011; He et al., 2012).

The second is whether flow-through or batch or mesocosm methodologies are used (Wagener et al., 2010). In the flow-through method, the extractant (e.g., seawater) is continuously passed through the filter with the samples. The flow-through methodology was developed to reduce the saturation effect on Fe dissolution (e.g., Buck et al., 2006; Wu et al., 2007; Ooki et al., 2009; Aguilar-Islas et al., 2010). Wagener et al. (2010) summarized the advantages and disadvantages of these two methods, which are summarized below. Flow through protocols have the advantage to be easy to handle and to bring information on the control of dust FFS by aerosol characteristics (Buck et al., 2006), but it has limitations in terms of marine biogeochemical perspectives, as the complex equilibrium between adsorption and dissolution that occurs during particle settling in the surface ocean is not taken into account. Batch experiments are more appropriate to investigate the processes that occur when atmospheric particles are mixed into the oceanic mixed layer. The disadvantage is that these experiments may be subject to another artefact, the adsorption of dissolved Fe on dust particles as demonstrated by Zhuang and Duce (1993). Mesocosms studies are difficult to handle, but they do better represent the natural conditions, particularly in considering the biological compartment and the biogeochemical characteristics of the large body of water enclosed inside the bags after the introduction of the particles (Wagener et al., 2010).

The third is the extraction time. In MilliQ water, the quasi-equilibrium is generally established relatively quickly, e.g., less than a few hours (e.g., Desboeufs et al., 1999; Deguillaume et al., 2010). In sea water, Fe in Sharan dust may continue to dissolve after 7 days (Wagener et al., 2008b). At low pH, Fe will continuously dissolve over a thousand hours (Trapp et al., 2010; Shi et al., 2011a). Under these circumstances, the choice of extraction time becomes important. The question of how to compare resultant FFS with those from other methods remains unanswered.

1.2. Use of soil samples as surrogates for dust in aerosol studies

Many studies that aimed to understand the processes controlling the FFS in mineral dust used samples of desert soils from various source regions (e.g., Guieu et al., 2002; Bonnet and Guieu, 2004; Lafon et al., 2006; Shi et al., 2009, 2011a,b). These samples, often called dust or dust precursors are generally size-sorted, to mimic dust collected in the atmosphere. The most commonly used size-sorting technique is wet sieving, where less than 20 μm particles can be obtained (e.g., Lafon et al., 2006; Shi et al., 2009). Wet sieving has the effect of wetting the surface of the aerosol/dust and will remove the most soluble and labile Fe fraction from the samples. Fortunately, unlike volcanic aerosols (Duggen et al., 2007, 2010), this process only remove small amounts of soluble Fe in the mineral dust. For example, Desboeufs et al. (1999) showed that less than 0.04% of Fe is dissolved at pH larger than 4. On the other hand, this is the most soluble and labile form in sea water. Sometimes, soil is re-suspended in a pre-cleaned air flow and subsequently the dry dust is collected with size-selective particulate matter (PM) samplers, in which PM_{10} (<10 μm) is often used to represent the atmospheric dust. The principal reason for using such samples is that they are available in large amounts (g – kg) compared to atmospheric dust, often only available in μg-mg amounts. This enables experiments to be carried out on the same dust-precursor from which results can be directly compared. In addition, such samples are clearly the precursor of atmospheric dusts *prior to uplifting* and thus have not been subject to

Author's personal copy

changes that can happen to mineral dust in the atmosphere, allowing them to be used to investigate how these properties are modified during simulated atmospheric processing. It appears that Fe mineralogical composition including the content of the most reactive Fe in the wet-sieved PM_{20} samples is not affected by the wet sieving process (Shi et al., 2011a; Lafon et al., 2006). Therefore, using such size separated soil samples is a practical and often necessary compromise relative to using atmospheric dust samples although it is preferable not to use wet sieving.

2. Analytical techniques used to study Fe in dust: an introduction

The key importance of Fe as a micro-nutrient in the world's oceans has sparked studies in many different disciplines including oceanography, atmospheric sciences, mineralogy, geochemistry, biogeochemistry, and biology. A wide range of methodologies have been used from nanometer-scale resolution imagery and chemical analysis in the laboratory, to large, regional-scale satellite observations aimed to help the development of Earth system models.

A review of methods and techniques used to determine the geochemical and mineralogical properties of Fe in dust is presented in Table 2. X-ray diffraction (XRD) has been used to identify and semi-quantitatively assess the mineral composition of dust particles (e.g., Merrill et al., 1994; Avila et al., 1997; Arnold et al., 1998; Shi et al., 2005; Shao et al., 2007, 2008; Shen et al., 2006b; Kandler et al., 2007, 2011). However, conventional XRD is often not sensitive enough to detect and *a fortiori* identify or differentiate between the different Fe oxides often due to the less crystalline structure (very broad peaks), overlap of the main diagnostic peaks of Fe oxides and the low amounts of such oxides in the samples (usually a few % in mass).

Sequential extraction of Fe by chemical reagents has traditionally been used to determine the amount of different Fe phases in a variety of geological materials including soils and sediments (e.g., Raiswell et al., 1994; Hyacinthe and Van Cappellen, 2004; Hyacinthe et al., 2006). The most widely used scheme is based on that developed by Kostka and Luther (1994) and Mehra and Jackson (1960) and includes ascorbate and dithionite extractions for extraction of Fe oxides. Hyacinthe et al. (2006) and Raiswell et al. (2008) combined these two methods and this is the method followed in Shi et al. (2009, 2011a,b). Ascorbate extraction (i.e., a deoxygenated solution of 50 g L^{-1} sodium citrate and 50 g L^{-1} sodium bicarbonate to which 10 g L^{-1} of ascorbic acid was added) dissolve the most reactive and poorly crystalline pool of Fe (FeA), often mainly composed of ferrihydrite (e.g., Kostka and Luther, 1994; Reyes and Torrent, 1997; Cornell and Schwertmann, 2003; Hyacinthe et al., 2006; Shi et al., 2009, 2011a; Raiswell et al., 2010). Dithionite extraction quantitatively solubilizes the remaining Fe (oxyhydr)oxides phases including goethite and hematite (FeD) (e.g., Raiswell et al., 2008). This method has been firstly developed and applied to dust by Lafon et al. (2004), which has been confirmed to be an important step in understanding the Fe mineralogical compositions and optical properties of mineral dust (Lafon et al., 2006; Redmond et al., 2010). A similar methodology is followed by Lafon et al. (2006), Formenti et al. (2008), and Shi et al. (2009, 2011a,b). Direct reflectance spectroscopy (DRS) can be used to quantify the ratio of hematite to goethite in a particular dust sample (Lafon et al., 2006; Formenti et al., 2008; Lazaro et al., 2008; Shi et al., 2011b). The content of hematite and goethite separately can then be calculated using the total Fe oxides content (FeD) if assuming FeD is predominantly hematite and goethite.

Table 1
Species and mineral forms of Fe.

Species or mineral	Chemical forms or definition
Dissolved	<200 or 450 nm in solution
Ferrihydrite	$Fe(OH)_3$
Goethite	FeOOH
Hematite	Fe_2O_3
Magnetite	Fe_3O_4
Cay minerals	Fe substituted in the clay lattice
Other aluminosilicate	Fe in mineral lattice

Note: dissolved Fe is usually defined as total Fe that passes through a filter with a certain pore size, for example, 0.2 or 0.45 μm.

Many different destructive and non-destructive methodologies have been used to measure the total Fe content (FeT) in dust samples (e.g., X-ray fluorescence (XRF) spectrometer and Particle-induced X-ray Emission (PIXE)) (Formenti et al., 2011 and references therein). Total digestion of dust samples by HF/HNO_3 mixtures following by chemical analyses also gives the total Fe content. Extraction by 6 N HCl or Aqua Regia gives total Fe except for the Fe contained in the most refractory mineral phases.

Most common techniques for direct observation of individual dust particles are scanning electron microscopy (SEM) coupled with energy dispersive X-ray spectrometry (EDX) and transmission electron microscopy (TEM) coupled with EDX, selected area electron diffraction (SAED) and electron energy loss spectrometry (EELS). Electron microscopic analysis provides size and high resolution morphology of individual particles down to nanometer-scale. SEM-EDX and TEM-EDX provides information on chemical composition of individual particles down to sub-micrometer and nano-meter size, respectively (Buseck and Posfai, 1999; Shi et al., 2003, 2009, 2011b; Posfai and Buseck, 2010). Combining analytical TEM with EDX and SAED, the mineralogy of individual dust particles may be identified (Buseck and Posfai, 1999; Shi et al., 2009, 2011b). TEM-EELS can be used to quantify the ratio of Fe(II)/Fe(III) (Garvie and Buseck, 1998) as well as the spatial distribution of different elements in individual nano-sized particles by EFTEM. Recently, synchrotron-based X-ray absorption spectroscopy (XAS) has been used to study the speciation of Fe in the aerosols. For example, Majestic et al. (2007) quantified the Fe(II)/Fe(III) ratio in size-separated aerosol samples while Ohta et al. (2006) and Schroth et al. (2009) used XAS to quantify Fe speciation in dust and/or other materials.

3. Processes in the dust source regions and their control on Fe mineralogy

In this section, we will firstly review our current understanding of the Fe mineralogy and speciation and the physicochemical properties of Fe minerals in the dust. We will then link the Fe mineralogy found in mineral dust with the weathering processes in the dust source regions.

3.1. Characteristics of Fe minerals in the dust

Mineral dust from desert regions typically may contain a mixture of several Fe-bearing minerals including: ferrihydrite and other poorly crystalline Fe phases (Shi et al., 2009, 2011a), crystalline hematite (Fe_2O_3), goethite (FeOOH) (Arimoto et al., 2002; Lafon et al., 2004, 2006; Shen et al., 2006a; Formenti et al., 2008; Journet et al., 2008; Shi et al., 2009), magnetite (Fe_3O_4) (Lazaro et al., 2008) and Fe-bearing clay minerals, such as illite, mixed layer illite/smectite, and smectite (e.g., Bergametti et al., 1989; Avila et al., 1997; Shi et al., 2005; Leinen et al., 1994; Merrill et al., 1994; Arnold et al., 1998) (Table 1). Although there are many primary Fe-containing minerals in primary volcanic and metamorphic rocks (e.g., amphiboles and pyroxenes), such Fe minerals are not identified in dusts (e.g., Merrill et al., 1994; Avila et al., 1997; Arnold et al., 1998; Shi et al., 2005, 2011b; Shao et al., 2007, 2008; Shen et al., 2006b; Kandler et al., 2007, 2011).

Author's personal copy

Table 2
Commonly-used methods for characterizing Fe in the dust.

Method	Expected information	Examples of references
XRD	Identity and semi-quantitative assessment of minerals	Merrill et al. (1994), Avila et al. (1997), Arnold et al. (1998), Shi et al. (2005, 2011b), Shao et al. (2007, 2008), Shen et al. (2006b), Kandler et al. (2007, 2011), references in Formenti et al. (2011)
Sequential extraction	Content of poorly crystalline and crystalline Fe oxides	Lafon et al. (2006), Formenti et al. (2008), Lazaro et al. (2008), Shi et al. (2009, 2011b)
DRS	Ratio of hematite to goethite	Lafon et al. (2006), Formenti et al. (2008), Lazaro et al. (2008), Shi et al. (2011b)
XRF/PIXE/INNA	Total Fe	Formenti et al. (2008), Shi et al. (2009, 2011a,b)
ICP-AES/ICP-MS	Total Fe/dissolved Fe in a solution	Baker et al. (2003, 2006a,b, 2007), Cwiertny et al. (2008a)
SEM-EDX/ TEM-EDX	Fe content and Fe spatial distribution in individual dust	Buseck and Posfai (1999), Shi et al. (2005, 2009, 2011b), Posfai and Buseck (2010), Chou et al. (2008), Kandler et al. (2007, 2009, 2011)
TEM and TEM-SAED	Fe mineralogical composition and crystal order in individual dust	Buseck and Posfai (1999), Shi et al. (2009, 2011b), Lieke et al. (2011)
TEM-EELS	Ratio of Fe(II)/Fe(III) in individual dust	No report to date
Synchrotron-based XAS	Ratio of Fe(II)/Fe(III) in total dust	Ohta et al. (2006), Schroth et al. (2009)
Mossbauer	spectrometry	Identification of Fe(II) and Fe(III) in total dust
Cwiertny et al. (2008a)		

Note: the definitions of the abbreviated methods are described in the main text.

The most labile form of Fe supplied to the ocean is dissolved Fe (Table 1), which are present in the dust and in rainwater (e.g., Heller and Croot, 2011; Baker and Jickells, 2006; Kieber et al., 2005; Willey et al., 2000, 2004, 2008, 2009). Dissolved Fe(II) in the rainwater was shown to remain stable for 4 hours and therefore is a potential source of bioavailable Fe (Willey et al., 2008). Amorphous Fe minerals including nanoparticles of ferrihydrite were highly reactive and potentially bioavailable (Nodwell and Price, 2001; Visser et al., 2003; Chen and Siefert, 2003). Amorphous Fe oxide particles have been identified in dust precursor samples and they generally exhibit a grain size in the nanometer range (Fig. 3a, Shi et al., 2011b). In dust from wet deposition collected in Western Mediterranean, ferrihydrite was also identified (Fig. 3b, Shi et al., 2009), but it was suggested that such ferrihydrite particles were formed during cloud processing. Shi et al. (2011a), Wagener et al. (2008b) and Deguillaume et al. (2010) all suggested that there was a highly reactive Fe pool in Saharan dust or urban particulate matter. Shi et al. (2011a) indicated that such highly reactive Fe pool in the Saharan dust samples has a reactivity similar to aged ferrihydrite. Nanoparticles may also be formed immediately after deposition by the interaction of dissolved Fe with seawater (e.g., Nishioka et al., 2005; de Baar et al., 2005). These newly formed or directly deposited nanoparticles (from rainwater) have a much higher dissolution rate than more crystalline Fe oxide minerals and therefore potentially more bioavailable (e.g., Nodwell and Price, 2001; Raiswell and Canfield, 2012).

The most abundant form of Fe oxides in dust or dust precursors are goethite and hematite (Lafon et al., 2006; Lazaro et al., 2008; Shi et al., 2011b). Goethite is by far the most common Fe oxides in soils and hematite is the second most common one (Cornell and Schwertmann, 2003). Goethite particles in soils are usually acicular but, unlike their synthetic counterpart, show defects, micropores and serrated edges (Cornell and Schwertmann, 2003). Similarly, some hematite in dust precursor samples show a grainy structure (Fig. 3c) like synthetic hematite, formed from ferrihydrite aggregates. This provides support for a similar mode of formation in dust as in soils (Cornell and Schwertmann, 2003). Sometimes, however, the conditions are not favourable for crystal growth and no specific morphology develops (Fig. 3d), although the particles are still Fe-rich.

The crystal size of Fe oxides in most natural soil samples ranges from a few nanometer to micrometer (Cornell and Schwertmann, 2003). This appears to be applicable to the soils from which the Saharan dust is produced (Fig. 3c and d) and for Chinese loess samples (Cwiertny et al., 2008a). Although the surface areas of Fe oxides in some soils have been estimated (Fontes and Wee, 1996), those in the dust or dust precursors are not known. It should be noted that generally synthetic and commercial Fe oxides are usually well crystallized with characteristic morphologies, larger size and well-defined surface area (e.g., Fig. 2e and f). This is because the formation conditions including pH, temperature, and ionic strength are well controlled (Cornell and Schwertmann, 2003). Such conditions are rarely found in a natural desert environment.

Clay minerals in dust also contain Fe which can under certain conditions transform to chemically available forms (e.g., Journet et al., 2008). In terms of reactivity, clay minerals are considered the most refractory Fe-containing minerals in dust (e.g., Merrill et al., 1994; Avila et al., 1997; Shi et al., 2011b; Shao et al., 2007, 2008; Shen et al., 2006b). The Fe content, even in the same type of clay mineral, e.g., illite, can be highly variable. For example, the illite standard sample used in Shi et al. (2011b) contained 22% and 66% more Fe than the two illite standards used in Journet et al. (2008) and Paris et al. (2011). This chemical heterogeneity is partly due to the parent/primary mineral from which the clay minerals originated and partly to differences in chemical weathering regimes in soils (Meunier and Velde, 2004). The relationship between Fe oxides and clay minerals in atmospheric dust is so far unclear. Both are formed during chemical weathering of parent minerals and are in intimate physical association with each other. Also, Fe oxide nanoparticles readily attach onto the surface of clay minerals (Lieke et al., 2011; Scheuvens et al., 2011; Raiswell et al., 2008; Kandler et al., 2007). Thus, some of the potentially available Fe in "standard" clay minerals used in previous works is likely to be the adsorbed Fe oxides particles, and Fe located at the edge of clay particles while the remainder is refractory Fe held in the clay lattice structure (Raiswell and Canfield, 2012; Shi et al., 2011b).

Evidence from SEM-EDX analysis of large numbers of individual dust particles suggests that Fe-rich dust particles are usually finer in size, e.g., <1 μm (Fig. 4a and b, see also Kandler et al., 2007; Chou et al., 2008; Coz et al., 2009). In the coarse (>1 μm) dust particles, weight percentage of element Fe is usually less than 20% (Fig. 4). These results suggest that most of the Fe-bearing coarse dust particles contain other elements, such as Ca and Si.

3.2. Fe mineralogy in North-African dust and soils and its regional variability

3.2.1. Fe oxide content

The Fe oxide content (the ratio of dithionite Fe (FeA + FeD) to total Fe (FeT)) in dust and dust precursors is an important parameter

Author's personal copy

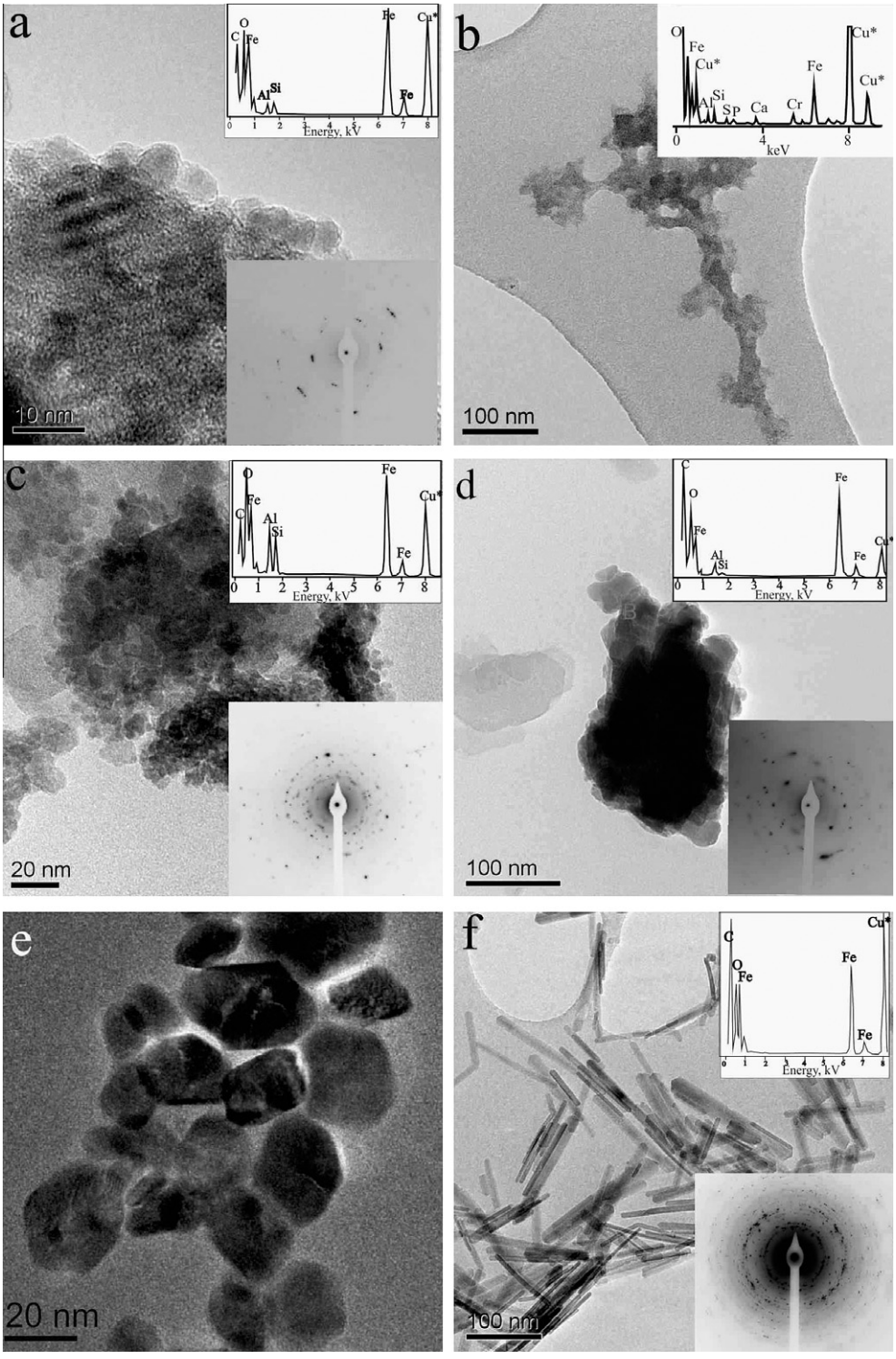

Fig. 3. Microscopic properties of Fe-bearing particles in dust precursor samples, the dust from a wet deposition sample, and synthetic highly crystalline Fe oxides. (a) TEM micrograph, EDX spectrum and SAED pattern of a poorly crystalline Fe oxide particle in a soil sample collected from Banizoumbou in Niger; (b) TEM micrograph of a nanoparticle aggregate in Saharan dust from a wet deposition sample with the corresponding EDX spectrum showing Fe as the dominant metal element; the Cu in the spectrum is from the Cu grid used as sample holder; (c) and (d) TEM micrographs, EDX spectra and SAED patterns of hematite and goethite particles in two soil samples collected from the Tibesti Mountains in South Libya and Banizoumbou in Niger; (e) TEM micrograph of a synthetic hematite sample; (f) TEM micrograph, EDX spectrum and SAED pattern of a synthetic goethite sample. Fig. 3a–d and f are reproduced from Shi et al. (2011b, 2009) and Fig. 3e from Kim et al. (2010) by permission of American Geophysical Union and American Chemical Society.

to characterize the Fe mineralogy (Lafon et al., 2004, 2006; Shi et al., 2011b). This parameter can be measured using the sequential extraction techniques mentioned in Section 2.

There appears to be a systematic trend in this ratio across N. Africa. Lafon et al. (2004) reported a lower ratio in the Saharan dust samples (0.44 ± 0.11) than in Sahelian dust samples (0.65 ± 0.04). Similar results have been reported by Lazaro et al. (2008), who showed that dust originating from the Saharan and Sahel region have a (FeA + FeD)/FeT ratio of 0.35 ± 0.07 and 0.58 ± 0.03, respectively (calculated from Table 3 in Lazaro et al. (2008)). Formenti

Author's personal copy

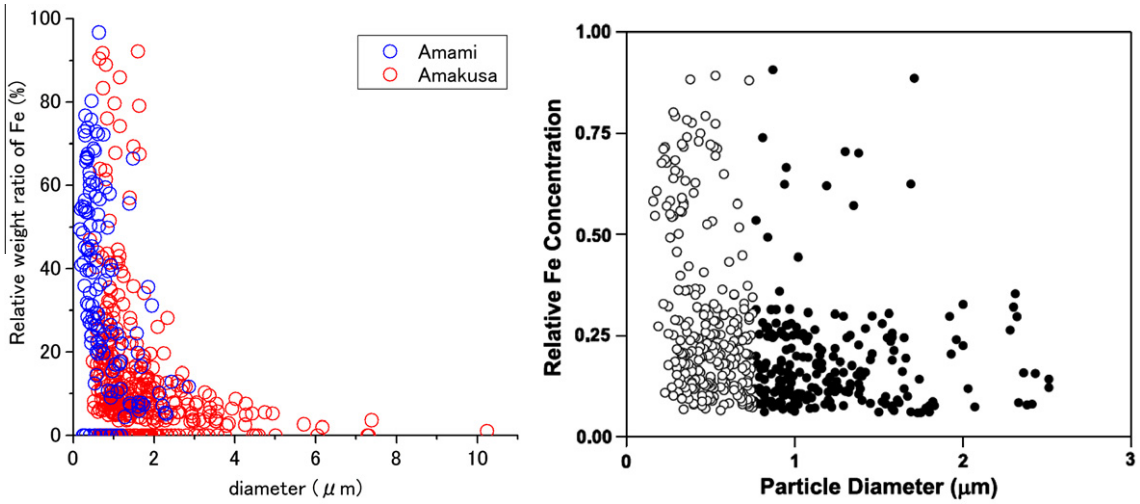

Fig. 4. Size dependence of Fe-content (weight percent) in individual Fe-bearing Asian dust particles collected at two sites, Amami and Amakusa in Japan (a) and in a dust-precursor sample (Chinese loess) (b). Solid and open circles in Fig. 4b represent the particles larger than 0.75 μm and less than 0.75 μm, respectively. Fig. 4a is reproduced from Ogata et al. (2011) with permission of the authors and Fig. 4b from Cwiertny et al. (2008a) by permission of American Geophysical Union.

Table 3
Data on Fe oxides content determined by chemical extractions in Saharan dust or dust precursor samples.

Samples[a]	Number of samples	Sources	FeA/FeT (%)	FeD/FeT (%)	(FeA + FeD)/ FeT	FeT (%)[b]	FeA/ (FeA + FeD) (%)	References
Sahara: dust precursors	2	Tibest Mountains, South Libya; Western Sahara	0.5 ± 0.2	35.3 ± 3.4	0.36 ± 0.04	4.7 ± 0.1	1.4	Shi et al. (2011b)
Sahel: dust precursors	3	Banizoumbou; Gourou Goussou; Giraffe Reserve at Koure (all in Sahel region and in Niger)	0.5 ± 0.4	55.8 ± 4.6	0.57 ± 0.04	5.7 ± 2.9	0.9	
Ephermal lake deposit: potential dust precursor	1	Mali	7.30	44.70	0.52	4.20	14.0	
Palaeolakes: dust precursors or potential dust precursors	4	Bodele Depression, Chad; Chott el Djerid, Tunisia; Wadi al Hyatt, Libya; Wadi Ash Shatti, Libya	1.5 ± 1.1	18.8 ± 10.1	0.20 ± 0.11	1.6 ± 1.3	7.4	
Beijing: dry deposition dust	1	Not known	1.7	22.3	0.24	3.50	7.1	Shi et al. (2011a)
E. Mediterranean: dry deposition dust[c]	1	Not known	0.9	35.1	0.36	2.81	2.5	Shi et al. (2009)
W. Mediterranean: wet deposition dust[d]	1	Not known	2.4	35.6	0.38	3.58	6.3	
Sahel, Niger: non-local aerosol[e]	9	Mainly from Chad basin	NM[f]	NM	0.44 ± 0.01	4.4 ± 0.6	NM	Lafon et al. (2004)
Sahel, Niger: Local aerosol	7	Sahel region	NM	NM	0.65 ± 0.04	5.5 ± 0.3	NM	
Zhenbaitai, China: aerosol[e]	4	Gobi desert	NM	NM	0.48 ± 0.03	5.4 ± 0.2	NM	
Cape Verde: aerosol[e]	3	Sahel	NM	NM	0.55 ± 0.03	2.9 ± 0.1	NM	Lafon et al. (2006)
	3	South Morocco	NM	NM	0.55 ± 0.04	3.2 ± 0.3	NM	
	3	Central Sahara	NM	NM	55 ± 0.03	3.2 ± 0.2	NM	
Niger: wind tunnel generated aerosols form soils	3	Banizoumbou near Niamey (Sahel region)	NM	NM	0.75 ± 0.01	4.6 ± 0.1	NM	
Tunisia: wind tunnel generated aerosols from soils	3	Maounanear Tataouin	NM	NM	0.58 ± 0.01	2.5 ± 0.1	NM	
China: wind tunnel generated aerosols from soils	3	Ulan Buh area, China	NM	NM	0.43 ± 0.01	2.1 ± 0.1	NM	
Canary Island: aerosol[e]	12	Saharan origin by back trajectory	NM	NM	0.35 ± 0.07	NM	NM	Lazaro et al. (2008)
	2	Sahel origin by back trajectory	NM	NM	0.58 ± 0.03	NM	NM	
Banizoumbou, Niger: aerosol[e]	Not shown	Not shown	NM	NM	0.59 ± 0.05	Unknown	NM	Formenti et al.(2008)

[a] For details of sample information, please refer to the original references.
[b] FeT is the mass percentage of total Fe in the bulk sample.
[c] A dry deposition sample collected in the East Mediterranean (Israel) after a dust storm event.
[d] A dust sample filtrated from the rainwater in the western Mediterranean.
[e] The sources of the aerosols were mainly based on back trajectory analyses as mentioned in the original papers.
[f] NM is not measured.

Author's personal copy

Table 4
The arithmetic mean ratios of Hm/(Hm + Gt) in dust or dust precursor samples.

	Asian			N. African					
	Dunhuang	Yulin	Tongliao	North Atlantic	Canary Islands (Saharan)	Canary Islands (Sahel)	Canary Islands (Sahara/Sahel)	Saharan	Sahel
Number of samples	29	32	22	9	12	2	5	2	3
Hm/Hm + Gt	0.36	0.37	0.32	0.48	0.52	0.45	0.39	0.42	0.49
Range					0.34–0.63	0.29–0.61	0.26–0.51	0.34–0.50	0.41–0.60
Source	Shen et al. (2006a)			Arimoto et al. (2002)	Lazaro et al. (2008)			Shi et al. (2011b)	

et al. (2008) also reported a high ratio in ground-based dust aerosol particles collected at Banizoumbou, in Sahel region. Finally, Shi et al. (2011a) reported a high (FeA + FeD)/FeT ratio in Sahel soil samples (0.57 ± 0.04) and intermediate ratio in Saharan soil samples (0.36 ± 0.04) but lower ratio in paleolake samples (from Bodele Depression) (0.20 ± 0.11). The data in Table 3 suggest a systematic difference in this ratio and hence in the extent of Fe weathering processing in dusts or soils in the Sahel region (higher degree of transformation of original Fe-bearing minerals into Fe oxides) compared to those in the Sahara (see Section 3.3). It needs to be mentioned that the Bodele Depression is a huge area with both paleolake sediment and the fluvial deposit from the mountains (e.g., the Tibesti Mountains) during episodic floods. Therefore, a specific sample from one site should not be considered as representative of the whole Bodele Depression (see the difference in composition of samples from Bodele in Shi et al. (2011b), Washington et al. (2009) and Bristow et al. (2010)).

Shen et al. (2006a) reported the Fe oxide content in Asian dust, which is close to the Saharan dust (note: not Sahelian dust). Based on a fitting technique, Takahashi et al. (2011) claimed that most Fe in a set of Asian dust samples is present in the illite and chlorite. This does not seem to agree with all the works mentioned above. In addition, Takahashi et al. (2011) obtained a best fitting without hematite and goethite. This does not seem to be likely because without goethite, the Asian dust, called "KOSA" in Japanese (literally "Yellow Sand") would not have a yellowish colour.

3.2.2. Ratio of poorly crystalline to highly crystalline Fe oxides

The ratio of the FeA/(FeA + FeD) has been used to characterize the ageing of Fe oxides (transformation of reactive Fe, e.g., ferrihydrite, to less reactive Fe oxides such as goethite and hematite). Shi et al. (2011b) showed that the FeA/(FeA + FeD) ratio is usually small in samples from the Sahel and Sahara, i.e., $\ll$0.1 (Table 3). However, during long distance fluvial transport before accumulating as dust source deposits (McTainsh, 1989), and especially during the deposition and accumulation of dust in ephemeral lakes, small amounts of ferrihydrite or poorly crystalline Fe oxides (FeA) may also form. One example is the sample from an ephemeral lake in Mali, which had a FeA/(FeA + FeD) ratio of 0.14. In addition, in paleolakes, ferrihydrite can be formed by digenesis and remain preserved together with large amounts of carbonate/silica. This is the reason for the higher FeA/(FeA + FeD) values observed in the paleolake samples (e.g., Bodele, Table 3) (Shi et al., 2011b).

3.2.3. Ratio of hematite to goethite + hematite

Since the light absorbance properties of hematite and goethite are different (Redmond et al., 2010; Lafon et al., 2006), it is important to know their contents in dust to better calculate the radiative properties of dust. In addition, the ratio of hematite to goethite + hematite (Hm/(Hm + Gt)) in dust may provide important information about the conditions during pedogenesis, particularly temperature and precipitation (Torrent et al., 2007). Shi et al. (2011b) suggested that higher ratios correlate with lower potential FFS (fractional solubility of Fe after 72 h contact with pH 2 sulfuric acid) in dust precursors. Hm/(Hm + Gt) in dust or dust precursors showed a large variation from <0.3 to >0.6 (Table 4). It was originally suggested that African dust contained more hematite while Asian dust was richer in goethite (Shen et al., 2006a; Arimoto et al., 2002). However, more recent data cast doubt on this simplified relationship since there are large variations in the ratio of Hm/(Hm + Gt) in North African dust and dust precursor samples (Lazaro et al., 2008; Shi et al., 2011b) as this depends primarily on the nature and history of the source soils.

3.2.4. Fe speciation (Fe(II) and Fe(III)) in dust

It is important to understand the speciation of Fe in the particular dust itself because the solubility of different species of Fe is different depending on the position and oxidation states in each mineral lattice. Fe(II) is in general more soluble than Fe(III). Dissolved Fe(II) in the dust, once dissolved in sea water, may be oxidized rapidly to Fe(III) or complexed with organics, which are at least partially bioavailable. As in Deguillaume et al. (2005), we use the term "Fe speciation" to refer to the relative proportions of the two oxidation states of Fe (+2 and +3) in the dust. There is only limited data on the speciation of Fe in dust aerosol particles. Synchrotron-based X-ray absorption spectroscopy (XAS) (Ohta et al., 2006; Schroth et al., 2009) and Mössbauer spectrometry (Cwiertny et al., 2008a) have been used to determine the Fe oxidation state and bonding environment in dust or dust source materials. Chinese loess has been shown to have a significant fraction of Fe(II) (47%: Ohta et al., 2006; and 33%: Schroth et al. (2009)). Cwiertny et al. (2008a) also showed the presence of Fe(II) in a Chinese loess sample. By contrast no Fe(II) was detected in the Asian dust samples (fraction <11 μm) collected during a super dust storm event in Beijing (Ohta et al., 2006) and in an African dust sample (Schroth et al., 2009).

3.3. Formation of secondary Fe minerals during chemical weathering

Mineral dust prior to uplift is produced by physical and chemical weathering in the source regions of primary and secondary minerals generally over long periods of time. These processes shape the properties of the dust precursors (the soil that the dust is produced from) and therefore determine the nature and amount of Fe in the dust. A particularly important process that is relevant for Fe mineralogy found in the dust is chemical weathering and the subsequent aging of Fe oxides.

Fe in the original Fe minerals is released initially as Fe^{2+}, which is rapidly oxidized to Fe^{3+} in the presence of oxygen and crucially water at the pH values (>2) commonly found in surface environments. The Fe^{3+} in turn immediately hydrolyzes to form solid but metasable Fe oxyhydroxides. Once formed, these Fe oxyhydroxides change with time to form crystalline Fe oxides and their high thermodynamic stability usually ensures that they persist for long

Author's personal copy

periods of time (Cornell and Schwertmann, 2003). Some of the Fe^{2+} and Fe^{3+} may enter into the structure of aluminosilicate minerals such as clay minerals, forming secondary Fe-bearing minerals. As soil develops, more and more of the primary and secondary Fe-bearing minerals decompose and the Fe of their lattice structure is converted to Fe oxides in the soil (McFadden and Hendricks, 1985).

In the context of this review, the chemical transformation from primary to secondary Fe minerals can be quantified by the changing ratio of Fe (oxyhydr)oxides (including amorphous Fe, hematite and goethite, FeA + FeD) to the total amount of Fe (FeT). As chemical weathering proceeds, poorly crystalline ferrihydrite (FeA) is converted into more stable Fe oxides, such as hematite and goethite (FeD). This FeA to FeD conversion process can be relatively fast at geological time scales and hence the amount of FeA remains low in the dust precursors while more stable Fe oxides accumulate. Fe in the clay minerals and other aluminosilicates can also dissolve and be transformed into oxides. Hence, as the weathering proceeds, the ratio of (FeA + FeD)/FeT gradually approaches unity (Leigh, 1996). These parameters have been widely used as an indicator of the maturity of a soil as a function of time (*chronosequence*) (Cornell and Schwertmann, 2003). Shi et al. (2011b) found a high degree of correlation (with $R^2 = 0.86$, Fig. 5) between the ratio of (FeA + FeD)/FeT in dust precursor samples from North Africa with the Parker weathering index (Parker, 1970) (Fig. 5), suggesting that the degree of chemical weathering in the source area determines the amount of Fe(III) oxides in the dust produced from that area.

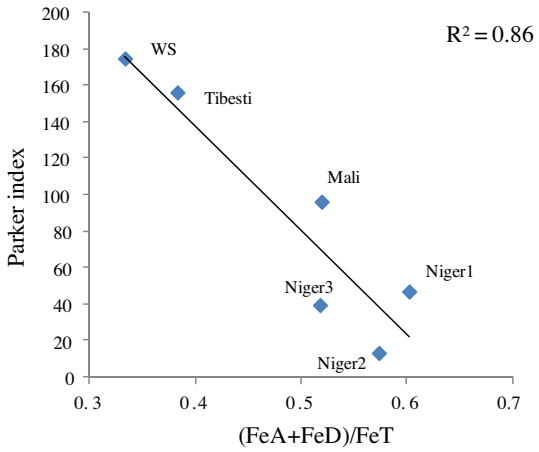

Fig. 5. Correlation of (FeA + FeD)/FeT with the Parker weathering index in Saharan and Sahel soil dust samples. A lower Parker index suggests a higher degree of chemical weathering. Adapated from data in Shi et al. (2011b).

4. Dust processes in the atmosphere and their impact on FFS

4.1. An overview of the atmospheric processing of dust

Atmospheric processes strongly affect and increase the measured FFS in aerosols (e.g., Mahowald et al., 2005, 2009; Baker and Croot, 2010; Sedwick et al., 2007; Chuang et al., 2005; Desboeufs et al., 2005).

There are a number of processes taking place in the atmosphere which may affect the Fe speciation and FFS in dust aerosol particles. These include gravitational settling, mixing with anthropogenic and biomass burning aerosols, uptake of acidic gases followed by hydration/hydrolysis onto mineral particles and chemical changes of the mineralogy of Fe-bearing phases themselves (Fig. 1). Probably the most important of the chemical changes is the change of pH in the solution surrounding dust particles (either in cloud droplet or wet aerosol). It is well known that the solubilization kinetics of Fe oxides and other Fe-bearing mineral phases are very sensitive to pH variations, with acidic solutions promoting dissolution (Cornell and Schwertmann, 2003). Other processes that can cause solubilization of Fe in mineral dust include photoreduction and the aqueous complexation and chelating effect of organic ligands such as oxalate and malonate (Cwiertny et al., 2008a; Wang et al., 2009; Xu and Gao, 2008). The effects of these processes are also pH sensitive.

Dust particles can act as cloud condensation nuclei (CCN), particularly after being aged in the atmosphere (e.g., Rosenfeld et al., 2001; Shi et al., 2008; Manktelow et al., 2010; Kumar et al., 2011). The interaction of dust particles with cloud water, or cloud processing, provides the main mechanism for uptake of acid gases in the atmosphere (Seinfeld and Pandis, 2006). Water droplets become saturated with CO_2 and if SO_x or NO_x are present in the atmosphere, both will dissolve into these water droplets. Both gases can be formed as a result of pollution and/or from natural processes. SO_x is commonly produced from the burning of fossil fuels particularly coal while anthropogenic NO_x comes from high temperature combustion. Natural SO_x is produced from the oxidation DMS (dimethyl-sulfide) and other natural reduced sulfur compounds while NO_x is produced in lightning. Acid gases such as SO_x, HCl and other acids can also be found in the atmosphere associated with volcanic eruptions. The uptake of these acidic gases can lower the pH of the cloud water. The pH of water in clouds usually ranges from 3.5 to 6 depending on the balance between acid gases taken up in the droplets and the chemical nature of the CCN. Carbonate will also buffer any acids in the droplets. In addition, dissolution of ammonia can also neutralize the acids and raise the pH of cloud droplets.

However, an important effect in the context of Fe solubilization in dust during atmospheric transport is that clouds often evaporate leaving only a thin film of aqueous electrolyte around each dust particle (e.g., Seinfeld and Pandis, 2006). This film of water (aerosol water) has significant different properties as compared to that in clouds (Table 5). Aerosol water is often very acidic compared to the cloud droplet. pH values of 2 or even lower are suggested for such aerosol films (Zhu et al., 1992; Meskhidze et al., 2003). In addition, this film of water exhibits a much higher ionic strength than cloud water, while simultaneously the dust-to-liquid ratio is drastically increased (reaching thousands of grams of dust per litre of water). This change in dust-to-liquid ratio may result in the adsorption of dissolved species to the particles, although its effect decreases at lower pH. Finally, clouds can form and evaporate several times (Seinfeld and Pandis, 2006), inducing, for the dust particles, five to ten cycles of pH alternation before being deposited via wet deposition or settled as dry materials to the ocean surface.

In the following sections, we will examine these processes as they affect the FFS in atmospheric systems. We will also examine the relationship between the mineralogy of Fe phases in dust particles and how that is affected and, at times, altered by these atmospheric processes. Because of the importance of Fe bioavailability in ocean carbon processes, we will finally consider how such processes can be better included into atmospheric models.

4.2. Gravitational settling

Chen and Siefert (2004) and Baker and Jickells (2006) have noted an inverse relationship between FFS in Atlantic aerosols and atmospheric dust concentrations (Fig. 6) with the lowest FFS associated with the highest particle concentration. Some more recent field data suggest a similar quasi-linear trend (e.g., Sedwick et al., 2007; Sholkovitz et al., 2009; Kumar and Sarin, 2010), but other studies do not, such as Buck et al. (2010b). Data reported from Trapp et al. (2010) indicated that while the highest FFS were found at the lowest dust loads, consistent with the data shown in Fig. 6, the FFS increased with increasing dust loading when the dust mass

Author's personal copy

Table 5
Differences in properties of water in the clouds and around the aerosols.

	Clouds	Aerosols	Selected references
pH	4–8	0–5	Deguillaume et al. (2005), Collett et al. (1994), Hegg et al. (2002), Straub et al. (2007), Falconer and Falconer (1980), Zhu et al. (1992), Meskhidze et al. (2003), Nenes et al. (2011), He et al. (2012)
Dust/water ratio	100 μg to 1 g/L	>5000 g/L	Sarthou et al. (2003), Baker et al. (2007), Ozsoy and Ornektekin (2009), Engelhart et al. (2011), Pikridas et al. (2010)
Ionic strength	Less than a few mmol/L	A few to 30 mol/L	Collett et al. (1994), Hegg et al. (2002), Straub et al. (2007), Zhu et al. (1992), Zhang et al. (2007), He et al. (2012)

concentration reached ~5 μg m^{-3} or more. Buck et al. (2010b) measured the FFS in 9 sets of size-fractionated aerosols collected in the North Atlantic Ocean during June–August, 2003. Their results showed that the aerosol FFS was somewhat variable with size but in general, it did not increase with decreasing particle size (Fig. 7).

Baker and Jickells (2006) explained the inverse relationship between dust mass concentration and FFS (open squares in Fig. 6) in terms of gravitational settling. They argued that the greater solubility at lower dust mass concentration could be due to a larger surface area to volume ratio of the finer dust particles. Baker and Croot (2010) later suggested that, based on field measurements, it may not be possible to unambiguously confirm that any of these effects is solely responsible for the relationship shown in Fig. 6.

More recently, Shi et al. (2011c) measured the size distribution of the FFS in the dust generated from two soil samples collected in the Saharan desert. Their results showed that the FFS in the dust generally increases with decreasing size. However, even the maximum FFS in the finest size fraction (0.18–0.32 μm) observed, which is only ~0.8%, is lower than most of the measured values in airborne aerosol samples previously reported (e.g., Chen and Siefert, 2004; Baker and Jickells, 2006). These results indicate that the size dependence of the FFS can at most explain a small part of the measured variability in FFS in atmospheric aerosol samples. The high values of the FFS of >1% in atmospheric aerosols samples are very unlikely to be seen in non-atmospherically processed dust particles (Hand et al., 2004; Mahowald et al., 2005) because of the refractory nature of the Fe in the original dust (Shi et al., 2011b).

4.3. Acid processing of dust

4.3.1. Effect of pH on the fractional Fe solubility in dust particles

Extensive studies in terrestrial/experimental systems show that the solubility of Fe oxides is highly dependent on the pH of the aqueous medium it is in contact with (e.g., Cornell and Schwertmann, 2003; Bonneville et al., 2009 and references therein). Especially at acidic conditions (e.g., pH <3), the solubility of Fe increases by a factor of ~1000 for each decrease in pH unit. In 1992, Zhu and co-authors proposed that acid dissolution in the aqueous thin film around dust particles is a major factor affecting the FFS. Although the pH of dust aerosol particles over the remote oceans has never been measured directly due to technical difficulty, theoretical calculations and model simulations suggested that aqueous electrolyte around dust aerosol particles can often have pH of less than 2, particularly in the finer dust particles (Zhu et al., 1992; Meskhidze et al., 2003, 2005; Solmon et al., 2009; Ito and Feng, 2010; Nenes et al., 2011). Motivated by the potential importance of acid dissolution in dust particles, a number of workers have sought to correlate the FFS with concentrations of acid species in aerosols from their field data (e.g., Hand et al., 2004; Baker et al., 2006a,b; Buck et al., 2010a; Hsu et al., 2010). The results have been ambiguous because it is difficult to measure or even estimate all of the aqueous species, or particle adsorption sites and then to predict the pH at high and variable ionic strength. Baker and Croot (2010) argued that the lack of a simple correlation between the bulk chemistry and the FFS in field data does not refute the importance of acidic processing as a major factor for increasing FFS in dust.

One of the potential factors to consider is the chemical heterogeneity of individual dust particles. It is known that mineral dust often contains a high percentage of carbonate (e.g., Chester et al., 1977; Shi et al., 2005; Formenti et al., 2011), which can neutralize the acid in contact with the dust. However, in practice, only some particles contain calcium carbonate and thus the acidification is only "neutralized" or buffered in carbonate-rich particles but not others. Most of the Fe-bearing dust particles also contain Si and Al and are thus presumably mainly clay minerals (Kandler et al., 2007; Scheuvens et al., 2011). Individual Fe-rich particles (e.g., Fe

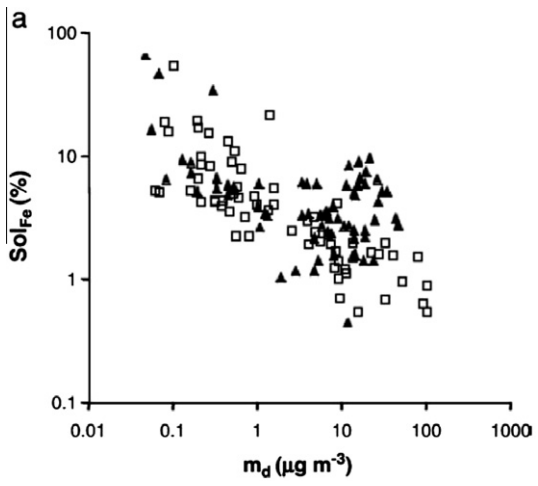

Fig. 6. Percentage of dissolved aerosol Fe as a function of mineral aerosol atmospheric concentration (m_d) over the Atlantic Ocean. The data were from Chen and Siefert (2004) (solid triangles) and Baker and Jickells (2006) (open squares). Note that the dust concentrations for the data of Chen and Siefert (2004) have been converted from total Fe concentration by assuming that dust contains 3.5 wt.% of Fe. Reproduced from Baker and Croot (2010) by permission of Elsevier.

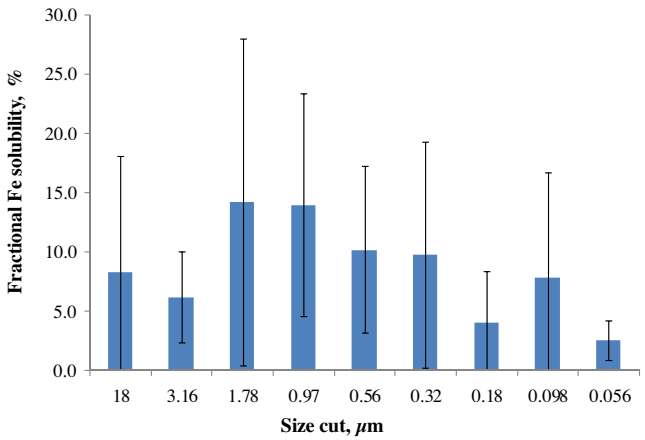

Fig. 7. Size dependence of the average FFS measured on 9 sets of size-fractionated aerosol samples collected over the North Atlantic Ocean. Error bars represent one standard deviation of the mean solubility percentage for each size fraction. Data were kindly provided by Dr. Buck from the University of California, Santa Cruz. Original data were published in Buck et al. (2010b).

Author's personal copy

weight percent >50%) are occasionally observed in both Asian and African dust (less of 3% in number of total observed particles) (Ogata et al., 2011; Coz et al., 2009; Kandler et al., 2007; Chou et al., 2008). If a 'dust storm' had come into contact with acid gases, although overall the pH may have been neutralized, that would not have been true for each individual dust particle and thus a pH induced increase in the FFS would still occur on those particles where acid gases caused decrease in pH. Sullivan et al. (2007) suggested that sulphate is preferably taken up on aluminosilicate Fe containing particles rather than the carbonate-rich particles, on which nitrate preferably deposit. This appears to support the acidification of Fe-rich but carbonate-free dust particles during transport although more work is needed to confirm this.

Furthermore Baker and Croot (2010) pointed out that the FFS enhancement during transport over the ocean occurs simultaneously with the deposition of acids onto dust particles and the removal of larger dust particles by gravitational settling. Thus, a simple correlation between acidic anion concentrations and FFS is unlikely. As a result of the difficulty in understanding field data, some of the important advances in quantifying the nature of acid-induced changes in the FFS of mineral dust have been carried out via laboratory experiments.

4.3.2. Laboratory based studies to understand the nature of pH control on Fe dissolution in dust

The first detailed studies of this type relevant to aerosols were carried out by Spokes et al. (1994) and Spokes and Jickells (1996). They found that dissolved Fe appeared in solution when a sample of Saharan dust was exposed to acidic solutions at pH 2 which is the pH relevant to wet aerosols (Fig. 8). Furthermore, when the pH of the solution was increased to 5–6, a range commonly measured in cloud water, the dissolved Fe concentration was considerably reduced (Fig. 8).

Subsequent work has expanded the pH range of such experiments and showed clearly that the dissolution of Fe in mineral dust is strongly pH dependant (e.g., Fig. 9, Mackie et al., 2006). Similar pH dependant Fe dissolution behaviour has been reported by Shi et al. (2011a) using both atmospheric dry deposited dust (Beijing dust) from Asia and dust-precursors (Tibesti) from Africa.

Cwiertny et al. (2008a) and Fu et al. (2010) also investigated the Fe dissolution behaviour of a series of soil and/or loess samples from pH 1 to 3 for up to 30 h. These authors demonstrated that, in addition to pH, the temperature, type of acids, photo-radiation and the nature of the dust all affect the Fe dissolution rates. Rubasinghege et al. (2010) also showed that the nano-sized goethite has a much larger dissolution rate than micrometer-sized goethite at low pH.

4.3.3. Dependence of potential fractional Fe solubility on Fe mineralogy and speciation

Schroth et al. (2009) showed that the FFS in mineral dust in MilliQ water is much lower than in glacial flour and coal fly ash. Cwiertny et al. (2008a) found a large difference in the FFS in dust surrogate samples from various deserts of the world. These results suggest that the nature of the mineral dust material has an important impact on its solubility.

A particularly important factor in controlling the amount of dissolved Fe during atmospheric transport is the original mineralogy of the dust. Journet et al. (2008) showed that commercial Fe oxide (goethite, hematite, and magnetite) samples have a much lower FFS (pH 2 for 2 h) compared to clay minerals. They argue that clay minerals are the main source of dissolved Fe in mineral aerosols. However, Shi et al. (2011b) and Raiswell and Canfield (2012) suggested that these differences can be explained, at least, in part by the poor reactivity of commercial Fe oxides (often large particles) and by the potential presence of Fe nanoparticulate and poorly crystalline (oxyhydr)oxide, formed during chemical weathering, associated directly with the clay mineral surfaces (see Section 3.1).

Shi et al. (2011b) investigated how the Fe mineralogy of a series of dust precursor samples from North Africa affects the FFS under acidic conditions. These dust precursor samples were collected from various locations representing different types of North African dust source regions including the main Saharan desert, the paleolakes, Sahel desert, and ephermal lakes. These results rendered a systematic relationship between the dust Fe mineralogy and the FFS (defined here as Fe_{psol}, which is the percentage of dissolved Fe in pH = 2 solution over 72 h to total Fe, and is a measure of the ease with which Fe in a given sample can be mobilized by atmospheric processes). Initially, poorly crystalline Fe (oxyhydro)oxides, as extracted by oxalate (FeO) or by ascorbate (FeA) (Reyes and Torrent, 1997) are formed. These are readily soluble under acidic conditions. In a natural sample, if aged, these reactive Fe phases may crystallize and convert into goethite and hematite, which are measured as (FeA + FeD) and are much less soluble (Fig. 10a). Fig. 10b shows that the FFS decreases with the ratio of (FeA + FeD)/FeT. Since (FeA + FeD)/FeT increases during the weathering of primary minerals, its inverse correlation with the FFS suggests that long or particularly intense chemical weathering in the source area tends to decrease the potential of the Fe to be solubilized once transported as dust in the atmosphere. However, the effects due to different source weathering regime is not big enough to explain the entire observed range of FFS (0.1–80%) in the atmospheric aerosols. This is supported by Paris et al. (2010) who showed that FFS in atmospheric African dust ranges from 0.1% to 3.4%.

4.3.4. Kinetics of Fe dissolution in dust

The dissolution kinetics and equilibrium solubilities of a large range of pure Fe oxides and oxyhydroxide mineral phases have been measured experimentally (Cornell and Schwertmann, 2003; Bonneville et al., 2009). However, these datasets cannot be directly applied in global dust models because dust samples are complex and variable mixtures of Fe minerals that have a variety of sizes and mineralogical and chemical compositions (Shi et al., 2011b). Furthermore, most studies on mineral dust only follow the Fe dissolution for a few hours to a few days. These experiments are designed to simulate the relatively short period of time during which atmospheric dust is potentially exposed to acidic pH. This design however prevented a fundamental understanding of the processes controlling Fe dissolution under acidic pH conditions to be

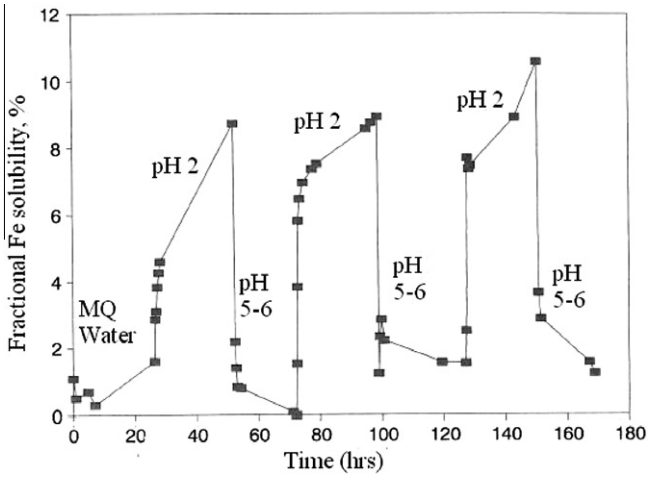

Fig. 8. Concentration of dissolved Fe over time during pH cycling using a Saharan aerosol (~30 mg L^{-1}). Reproduced from Spokes et al. (1994) with permission from Elsevier.

Author's personal copy

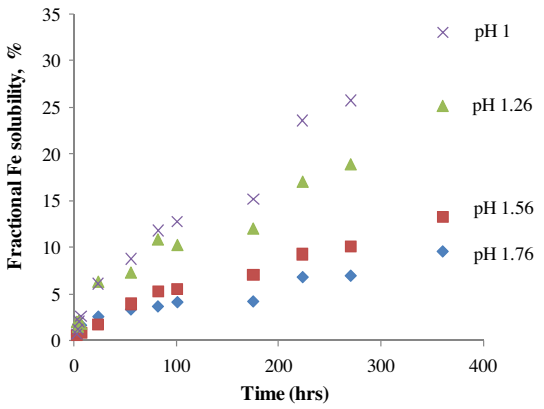

Fig. 9. Effect of pH on the release of Fe from Australian dust with time. Figure was produced from data provided by Doug Mackie from the University of Otago and the original figure was published in Mackie et al. (2006).

achieved. Recognizing these problems, Shi et al. (2011a) measured the Fe dissolution kinetics of representative dust and dust precursor samples in acidic conditions for longer periods of time than done before in the atmospheric literature in an attempt to measure both the Fe dissolution kinetics and Fe concentrations to reach dissolution plateau (i.e., a quasi-equilibrium values). The results on the concentration curves over time were then fitted to a series of geochemical models. Modelling results showed that the time-dependant Fe concentration were best described by three acid-extractable Fe pools each dissolving according to a (pseudo)-first-order kinetic pathway (Fig. 11). The dissolution rate constant k (h^{-1}) of each pool was independent of the source of the dust and its grain size (PM_{20} PM_{10} or $PM_{2.5}$). The "fast" Fe pool had a k (25 h^{-1} for pH 1) of similar magnitude to pure ferrihydrite nanoparticles and/or other poorly crystalline Fe(III) oxyhydroxide, while the "intermediate" and "slow" Fe pools had k values respectively 50–60 times and 3000–4000 times smaller than the "fast" pool. The "slow" Fe pool may consist of both crystalline Fe oxide phases (i.e., goethite and/or hematite) and Fe associated with clay minerals. In the samples analyzed, the initial mass of the "fast", "intermediate" and "slow" Fe pools represented respectively about 0.5–2%, 1–3% and 15–40 % of the total Fe in the dust samples (Shi et al., 2011a). These results are based on typical Saharan and Asian dust samples and the corresponding values may be different in samples from paleolakes, Sahel regions or other dust source regions.

The argument that dissolved Fe from more reactive Fe pool is mainly from the highly reactive Fe pool initially is supported by the results in urban particulate matter in Deguillaume et al. (2010) and Saharan dust in Wagener et al. (2010). However, Paris et al. (2011) argued that this is not the case although these authors appeared to agree that highly reactive Fe is more soluble. Their argument can only be valid if there is no pool of highly reactive Fe in their samples. But Paris et al. (2011) did not measure the content of highly reactive Fe in the dust samples. They also did not determine the dissolution or FFS in the highly reactive Fe (similar to aged ferrihydrite) and calculate the Fe potentially dissolve from the highly reactive Fe pool in the dust or the dissolution kinetics. A possible explanation of the abovementioned contradiction is that the calculation in Paris et al. (2011) is based on a debatable assumption that "standard" Fe minerals are representative of the similar minerals in the actual dust (see Section 3.1; Raiswell and Canfield, 2012; Shi et al., 2011b).

4.3.5. Importance of dust/liquid ratio as a control for Fe solubilization in dust

For practical reasons, laboratory experiments to quantify acid processes in dust systems were usually performed at relatively low dust/liquid ratios (in grams or milligrams of dust per litter of solution). Spokes and Jickells (1996) found that the FFS is independent of dust/liquid ratio <20 mg L^{-1}. However, at higher dust/liquid ratio, proportionately, less Fe is dissolved (Fig. 12). Similar results were also found by Mackie et al. (2006) and Shi et al. (2011a) using a maximum of 1 g L^{-1}. These dust/liquid ratios are approximately 3 orders of magnitude smaller than what is expected in dust aerosol particles (Table 5), where the dust/liquid ratio is likely to be more than 5000 g L^{-1} (Pikridas et al., 2010; Engelhart et al., 2011).

The important but previously unconsidered effect of this high dust/liquid ratio has been raised by Shi et al. (2011a) who calculated that, at much higher dust/liquid ratios (e.g., 3000 g L^{-1}), the high Fe concentration from the fast pool may suppress the dissolution of other Fe phases from the dust. Since it is not possible to experimentally measure the dissolution kinetics at typical dust/liquid ratio (>3000 g L^{-1}) directly in simple laboratory batch experiments, further work combining smog chamber experiments and/or theoretical calculations are needed to further understand the implications of this dust/liquid ratio to the natural system.

4.4. Cloud processing and photoreductive dissolution of Fe in dust

Properties of cloud water are fundamentally different to those of aerosol electrolyte solutions. For example, higher pH (>4), lower dust/liquid ratio (<50 mg L^{-1}) and lower ionic strength (< a few mmol L^{-1}) are usually found in cloud water than in aerosol water (Table 5).

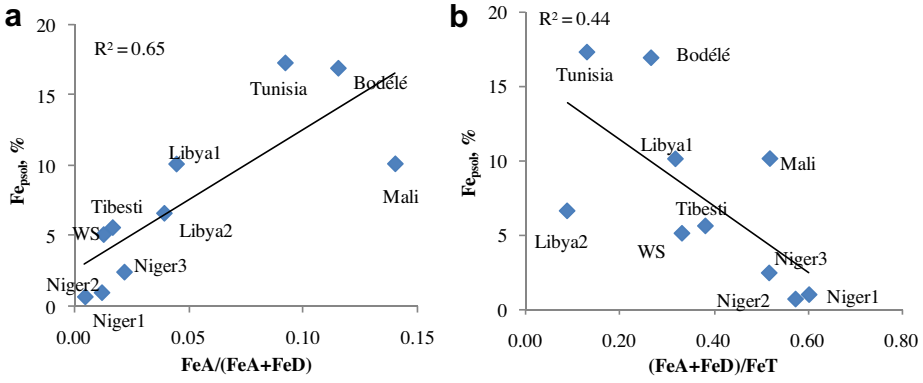

Fig. 10. Correlation of potential Fe solubility (Fe_{psol}) with (a) (FeA + FeD)/FeT; (b) FeA/(FeA + FeD) for soil dusts. Each data point represents a sample name. Tunisia, Bodele, Libya1 and Libya2 samples are from palaeolakes; Tibesti sample is from a flash flood river bed the Tibesti Mountain in Southern Libya; WS sample a palaeosol sample is from Western Sahara; Niger1, Niger2, and Niger3 samples are surface soil sample from Niger; and Mali sample is an ephemeral lake sediment from Mali. Reproduced from Shi et al. (2011b) with permission of American Geophysical Union.

Author's personal copy

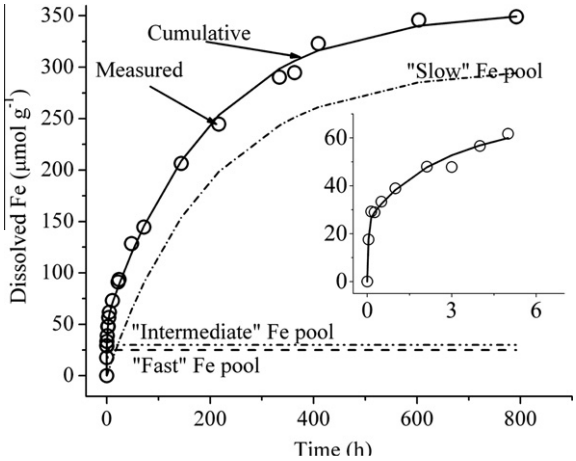

Fig. 11. Measured Fe dissolution kinetics (open circle) compared with the predicted curve (solid) of the Tibesti-$PM_{2.5}$ sample at pH 1, at a dust/liquid ratio of 60 mg L^{-1} assuming a 3-Fe pool model. The inset shows the measured Fe compared with the calculated Fe from the 3-Fe pool over the first 6 h of the experiments in more detail. Adapted from Shi et al. (2011a). Reproduced with the authors.

Spokes and co-authors (1994) were the first to notice that the FFS in dust decreases to a very low value (e.g., <0.5%) when the pH of the solution was increased to 5–6 to simulate cloud pH (Fig. 8). This was later confirmed in Mackie et al. (2005). Desboeufs et al. (1999) measured the dissolution rates of trace metals including Fe in wind transported Saharan dust samples from pH 3.8–5.3 at a dust/liquid ratio of 5 mg L^{-1} with a rather small fraction of the total Fe (<0.1%) being dissolved (Fig. 13). Desboeufs et al. (2001) further examined the factors influencing aerosol solubility during cloud processes and showed that the FFS depended only on the pH conditions of the last cloud cycle. Mackie et al. (2005) measured the Fe dissolution rates of an Australian dust sample across a larger pH range (pH 2.15 to ~7) and concluded that Fe is only significantly mobilized below a threshold of pH ~3.6 (Fig. 13).

It appears that Fe dissolution reaches a plateau (equilibrium) relatively quickly in the dust suspensions at pH larger than 4, for example, in 60 min (Fig. 14) (Desboeufs et al., 1999).

Shi et al. (2009) simulated the acid and cloud processing of dust samples following Spokes et al. (1994). Using high resolution microscopic techniques, Shi et al. (2009) found that increasing the pH from 2 to 5–6 in dust suspensions resulted in the precipitation of Fe nanoparticles of ferrihydrite, thus explained the lower measured FFS at pH of 5–6 in Fig. 8. This was observed directly by electron microscopy and confirmed by sequential Fe extraction of the soil samples which indicated an increase in the proportion of chemically reactive Fe extractable by an ascorbate solution after simulated cloud processing. Similar Fe-rich nanoparticles were also observed in wet deposited Saharan dusts from the western Mediterranean confirming that these processes also occurred in nature (Fig. 3b). Interestingly, ferrihydrite nanoparticles were not observed in dry-deposited dust from the eastern Mediterranean, and the sequential extraction of these dust samples revealed a higher content of reactive Fe (FeA, Table 3) in the wet-deposited dust from the W Mediterranean compared to that of the dry-deposited dust. These results suggest that the cycles between cloud-aerosol modes can trigger neo-formation of nano-size Fe particles and an increase in Fe reactivity in the dust.

4.4.1. Photo-reduction and organic complexation

It has long been known that it is possible to photo-reduce solid Fe oxides in solution to form dissolved Fe^{2+} under the conditions of UV light at relatively low pH, e.g., <4 (e.g., Faust and Hoigne, 1990). Laboratory simulations suggest that a steady state concentration of Fe^{2+} was quickly established (hours) during exposure of dust suspensions to solar radiation (Zhu et al., 1993; Spokes and Jickells, 1996). However laboratory simulations of photo-reductive dissolution of Fe in dust suggest that photoreduction when acting alone has limited impact on the total dissolved Fe concentration (thus FFS). For example, Zhu et al. (1993) found that less than 1% of the total Fe in Saharan dust aerosol particles could be photo-reduced to Fe^{2+}. Spokes and Jickells (1996) found that dissolved Fe comprised only 0.9% and 0.25% of the total Fe under light and dark conditions, respectively. This compares to >5% due to acid processing after 72 h at pH 2 (e.g., Spokes et al., 1994). Finally, Fu et al. (2010) showed that photo-reductive dissolution of Fe in surrogate dust sample suspensions at pH 2 only increases the FFS slightly, with the Arizona Test Dust showing the biggest increase from about ~4.5% to 5.5% after 12 h (Fig. 15). These results suggest that although photo-reductive dissolution may be important in enhancing FFS in mineral dust in the clouds, its effect on the total dissolution of Fe from the mineral matrix appears to be less dramatic (Zhu et al., 1993; Spokes and Jickells, 1996; Paris et al., 2011) when compared to the observed change in FFS in atmospheric aerosols from 0.1% at high dust mass concentrations to 80% at low concentrations (e.g., Mahowald et al., 2005; Baker et al., 2006a,b). The effect of photo-reduction on Fe dissolution, however, may be larger in anthropogenic aerosols (Siefert et al., 1994; Spokes and Jickells, 1996; Upadhyay et al., 2011), potentially because of the difference in mineralogy and speciation of Fe and/or the presence of organic matter in the material (Faust and Zepp, 1993; Pehkonen et al., 1993; Spokes and Jickells, 1996; Desboeufs et al., 2005; Schroth et al., 2009; Upadhyay et al., 2011).

Furthermore, processing of dust particles in the ice clouds might be efficient in solubilizing Fe after photoradiation because this process has been shown to be able to efficiently mobilize Fe in the synthesized hematite (Kim et al., 2010). However, further laboratory experiments to confirm this is needed.

Organic ligands such as formate, acetate and oxalate are found in atmospheric particles and clouds (Ervens et al., 2011; Marinoni et al., 2004; Gioda et al., 2009; Hegg et al., 2002; Straub et al., 2007) and they are able to form complexes with dissolved Fe and thus may increase the FFS in atmospheric waters. Complexation of Fe^{3+} by such ligands can also promote the photo-production to Fe^{2+}, which increases the FFS in the dust (Erel et al., 1993; Zhu et al., 1993; Pehkonen et al., 1993; Siefert et al., 1994). This area of research has attracted large interest recently. Xu and Gao (2008) suggested that oxalate adsorbed onto hematite can increase the dissolution rate by about an order of magnitude. Cwiertny et al. (2008b) investigated the oxalate assisted dissolution of goethite at low pH (pH 3). Paris et al. (2011) examined the impact of oxalate on dissolution of Fe from dust surrogate samples collected from the Sahara. Their results showed that the FFS increases from 0.0025% to 0.26% when oxalate concentration was changed from 0 to 8 μM (Fig. 16). Although the effect of oxalate on dissolved Fe concentrations in clouds is not large enough to explain the variability of field-measured FFS in atmospheric aerosols (ranging from 0.1% to 80%), this effect is as large as two orders of magnitude and thus a potentially important process to be considered in global models. Lastly, macromolecular organic ligands, such as humic-like substances originated from the soil degradation, which are found in surface river waters (e.g., Stolpe et al., 2010) and may be present in rainwaters (Muller et al., 2008, 2010), however, have great potential in complexing with Fe at intermediate pH conditions relevant to cloud waters. This remains to be investigated.

5. Modeling the impacts of atmospheric processing of dust on fractional Fe solubility

A number of modelling studies have been conducted to understand how different atmospheric processes affect the Fe

Author's personal copy

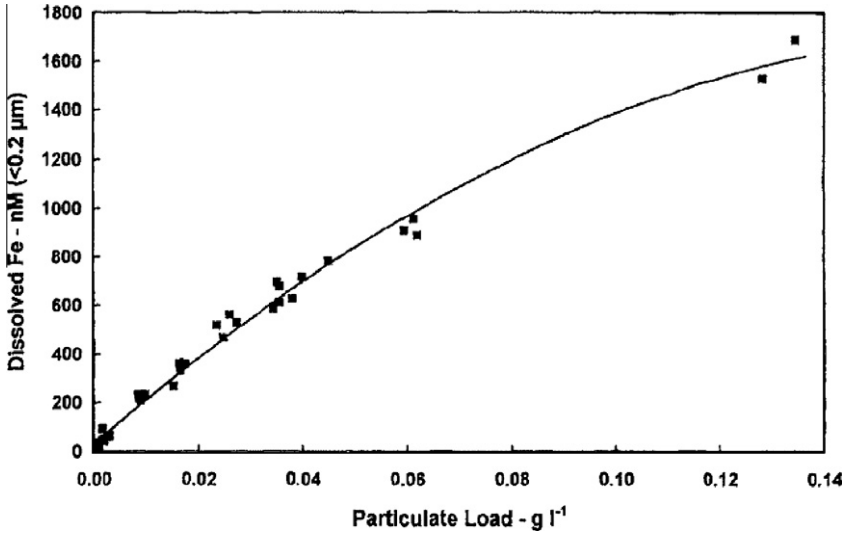

Fig. 12. Dissolved Fe concentration (<0.2 μm) after 4 h at pH 2 as a function of Saharan aerosol loading in g L^{-1}. Reproduced from Spokes and Jickells (1996) with permission of Springer.

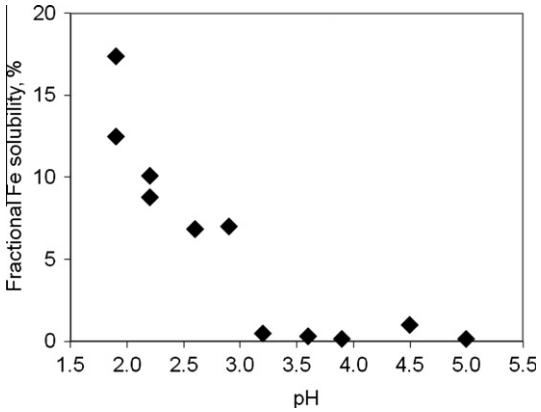

Fig. 13. FFS after 120 h extraction at varying pH shows that a threshold value for negligible extraction occurs at pH 3.2–3.6. Figure is produced from data provided by Doug Mackie from the University of Otago. Original data of this paper are published in Mackie et al. (2005).

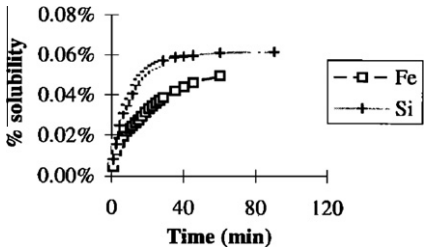

Fig. 14. Solubilization of Fe and Si over time at pH 4 from a Saharan dust sample (5 mg L^{-1}). Figure reproduced from Desboeufs et al. (1999) by permission of American Geophysical Union.

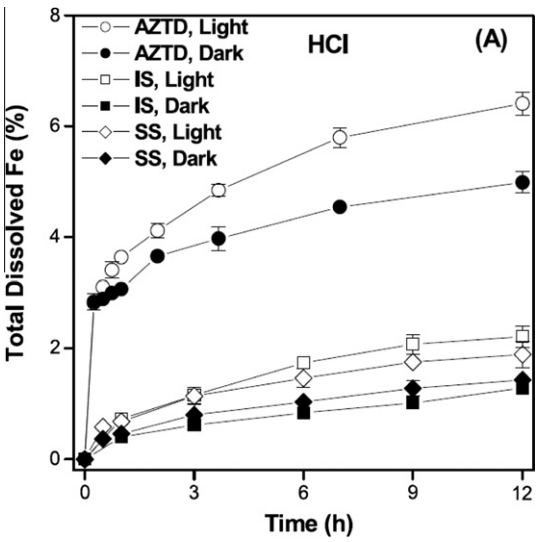

Fig. 15. Comparison of FFS as a function of time in suspensions of AZTD (Arizona Test Dust), IS (source material from inland of Saudi Arabia desert), and SS (source material from Saharan desert) in 0.01 N HCl (pH = 2) under irradiation and in the dark. Reactors contained a solids loading of 12, 12, and 3 g/L for IS, SS, and AZTD, respectively. When present, uncertainties represent one standard deviation from triplicate experiments. Reproduced from Fu et al. (2010) with permission from American Geophysical Union.

solubilization in the dust during transport. The processes which have been examined include cloud processing, acid processing, heterogeneous uptake of SO_2 on dust, photo-reduction, and gravitational settling. The first paper that included dust FFS in a model was published in 2004 by Hand and co-authors, who tested two simple hypotheses that FFS increases once the dust is (1) exposed to solar radiation and (2) being processed in the clouds. Luo et al. (2005) then simulated the effects of cloud processing, SO_2 heterogeneous reaction on dust, and sulphate heterogeneous reaction on dust on the FFS. Both models were able to reproduce the observed higher average FFS in dust particles transported for longer distances. However, because of the limited observations and/or laboratory reaction rates available, these models could not evaluate the relative importance of different mechanisms in matching available observations.

More recent works focused on the acid processing in the atmosphere as a potentially important reaction in controlling the amount of bioavailable Fe supplied to the ocean (e.g., Meskhidze et al., 2005; Luo et al., 2005; Fan et al., 2006; Solmon et al., 2009; Ito and Feng, 2010; Johnson et al., 2010; Moxim et al., 2011; Ito, 2012). Several models have been developed (e.g., Meskhidze et al., 2005; Luo et al., 2005; Fan et al., 2006; Solmon et al., 2009; Ito and Feng, 2010; Johnson et al., 2010). These models

Author's personal copy

were based on calculated aerosol pH values and the FFS was simulated from the dissolution rate of laboratory-made or commercial Fe oxides (i.e., hematite). Using the best data available at the time, Meskhidze et al. (2005) applied a three-stage Fe dissolution kinetic parameterization based on experimental rates for hematite.

Meskhidze et al. (2005) included the effect of photoreduction by assuming that the net daytime rate of hematite dissolution was 5–10 times greater than that at night. In their simulations, the effect of dust/liquid ratio was considered by applying a function of Gibbs free energy and the effect of pH was considered by including a function of the activity of H^+. Similar parameterization was followed in Luo et al. (2005), Solmon et al. (2009), Johnson et al. (2010), Ito and Feng (2010) and Ito (2012). The latter authors also considered the dissolution of Fe from illite in addition to hematite and the mixing state of Fe with carbonate in individual dust particles. They found that a significant amount of Fe (1–2%) can only be dissolved from hematite in the dust when the hematite is externally mixed (physically separated) from the carbonate in individual dust particles. Fan et al. (2006) used a simpler parameterization assuming zero-order dissolution of hematite, which did not consider the effect of pH changes or the dust/liquid ratio effect.

These models have all been able to successfully capture the observed higher FFS in dust collected above the open ocean compared to that observed close to the dust source area (Hand et al., 2004; Meskhidze et al., 2005; Luo et al., 2005; Fan et al., 2006; Solmon et al., 2009; Ito and Feng, 2010; Moxim et al., 2011). They also showed that incorporation of the acidic processing of Fe in the dust significantly affects the global distribution of the bioavailable Fe deposition fluxes to the oceans (e.g., Fan et al., 2006; Solmon et al., 2009; Ito and Feng, 2010; Moxim et al., 2011; Ito, 2012).

Most dust Fe dissolution parameterizations used in current models were based on experiments on laboratory-made or commercial ferric oxides particles (e.g., Azuma and Kametani, 1964; Zinder et al., 1986). These models, except in Ito and Feng (2010) and Ito (2012), also assumed that hematite is the only Fe mineral and that hematite particles are of single or similar size. These Fe dissolution schemes as well as the assumptions are debatable. Shi et al. (2011a) compared the actual Fe dissolution curves of representative dust samples to those predicted based on the present model parameterizations (Fig. 17). The figure shows that the Fe dissolution kinetics predicted by the parameterizations used in those models are largely under-estimating the measured Fe solubilization in the initial phase (i.e., <~40 h, Fig. 17). This is important as the very beginning of Fe dust dissolution is most relevant for aerosol processes.

Recent laboratory work on the dissolution of Fe from dust by acid processing, particularly from the most reactive Fe pool summarized above (Section 4.3.4) should be incorporated in the atmospheric models, as they may be able to increase the accuracy of these models (Luo et al., 2005). It is important that future experimental work is focused on providing the data and parameterization required for the next generation of climate models. The combined skills of low temperature geochemists and atmospheric modelers represent a powerful combination, which together will improve the accuracy of atmospheric models and thus our ability to reliably predict the effect of global climate and environmental change in the future.

In addition to the abovementioned atmospheric processes, gravitational settling has been hypothesized as a cause for the observed increase in FFS with decreasing dust mass concentration (Baker and Jickells, 2006). Shi et al. (2011c) combined the laboratory-measured FFS in size-segregated dust aerosol particles with model simulated size-resolved dust mass concentration over the North Atlantic Ocean. These authors estimated the impact of gravitational settling of dust particles on their FFS (Fig. 18). The results, particularly the sensitivity test, clearly showed that once the dust reaches the Atlantic Ocean, physical size sorting is not the dominant mechanism causing the enhancement of the FFS in dust particles during transport (e.g., Hand et al., 2004; Baker and Jickells, 2006). It was reported that very large particles (e.g., >20 μm) can be transported for long distances (e.g., Jaenicke and Schutz, 1978; Reid et al., 2003), but global models including GLOMAP that was used in Shi et al. (2011c) usually underestimate the transport distance of such large particles. This caveat in the model does not affect our conclusion though because the calculated fractional solubility would have been smaller if the transport distance of large particles were better simulated in the model. Shi et al. (2011c) further suggested that processes such as chemical reactions on the dust particles and/or mixing with anthropogenic particles are the dominant causes for the changes in FFS in transported dust.

On the other hand, it should be noted that during long-range transport, the shift in size will also likely be accompanied by relevant changes which include: (1) increase in the content of

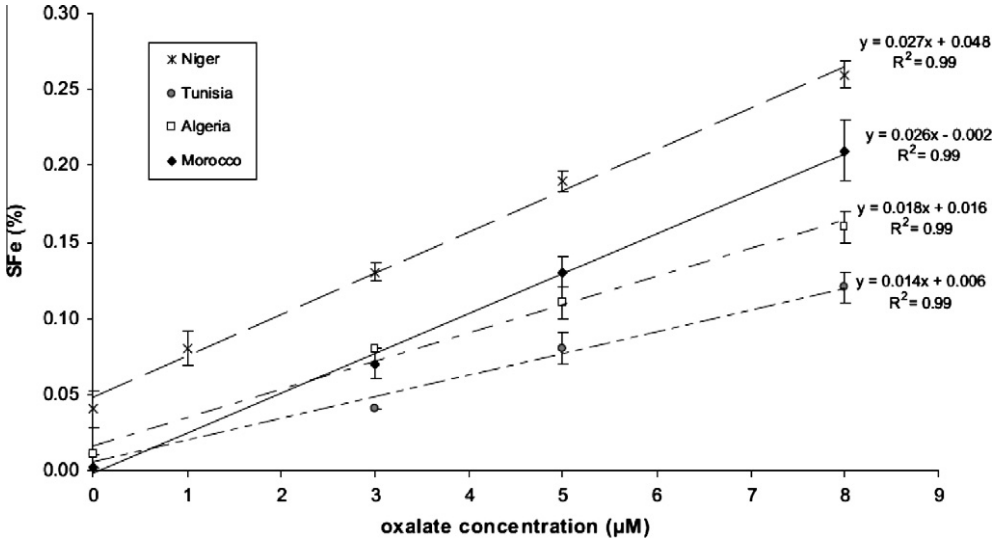

Fig. 16. Comparison of soluble iron with oxalate concentration for different source materials. Reprinted from Paris et al. (2011) with permission from American Geophysical Union.

Author's personal copy

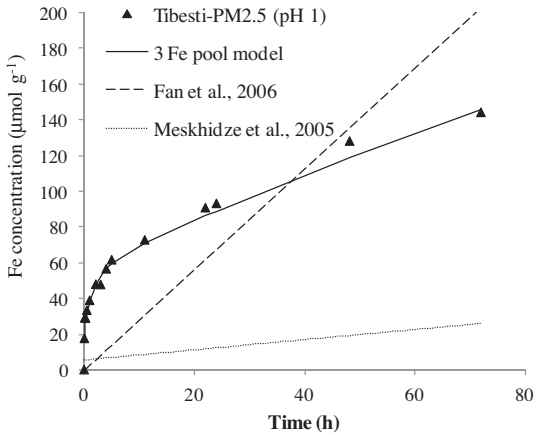

Fig. 17. Fe dissolution curves predicted from rate constants used in Meskhidze et al. (2005) and Fan et al. (2006), and the actual measured dissolution rates for Tibesti-$PM_{2.5}$ at pH 1 at 60 mg L^{-1}. Reproduced from Shi et al. (2011a) with permission of the authors.

more reactive Fe per mass of dust (Shi et al., 2011b); (2) increase in surface area (Baker and Jickells, 2006); and (3) reduced neutralizing capacity (less carbonate in the atmosphere) and thus increased potential for acid processing, photo-reduction and ligand promoted Fe dissolution (Spokes and Jickells, 1996). All these processes could potentially lead to an enhanced FFS in dust aerosols.

6. Summary and future work

Fe is a critical micronutrient for the ocean phytoplankton and Fe in the dust plays an important role in the global biogeochemical cycles and the climate system. However, Fe in the dust is extremely complex and in this review we only summarized the current knowledge in the forms and mineralogical compositions of the atmospheric dust or dust precursors and the factors that control them. We also provided a synthesis of the current understandings on how atmospheric processes affect the FFS in the dust. Important points from the above discussions are summarized in the following:

1. Dust contains a range of Fe minerals from poorly crystalline Fe oxides, crystalline Fe (oxyhydr)oxides such as goethite and hematite and all the way to clay minerals including illite, smectite, illite/smectite mixed layer, and chlorite. The solubilities of these Fe minerals vary by orders of magnitude.
2. Existing data suggest that the fraction of Fe oxides to total Fe in dust shows a regional variability in North Africa, with higher values being observed in the Sahel regions, intermediate values in the main Saharan desert and lower values in palaeolakes. These differences are caused by the variability in the degree of chemical weathering in the source areas. More data on the Fe mineralogical composition from the dust source regions, particularly the Asian dust source regions, are needed to provide a better constraint for global models.
3. Dust particles may be cycled between clouds, in which pH is usually higher than 4, and aerosols, in which pH can be substantially lower, e.g., 2. This cycle could happen several times before the particles are being removed from the atmosphere. Laboratory simulation of acid dissolution of Fe in dust showed that more Fe is solubilized at lower pH. However, the application of the acid processing of Fe in dust in the current models is impeded by the simplistic assumption of the Fe mineralogical compositions in dust and particularly the lack of dissolution rates under realistic conditions. The presence of three Fe pools with substantially different reactivity should be considered in the models. In addition, more geochemical and multidisciplinary measurements combined with modelling should be conducted to provide more realistic formation constants for Fe complexes with both organic and inorganic ions and the reaction rates at conditions relevant to dust aerosol particles, e.g., high ionic strength, high dust/liquid ratio and low pH.

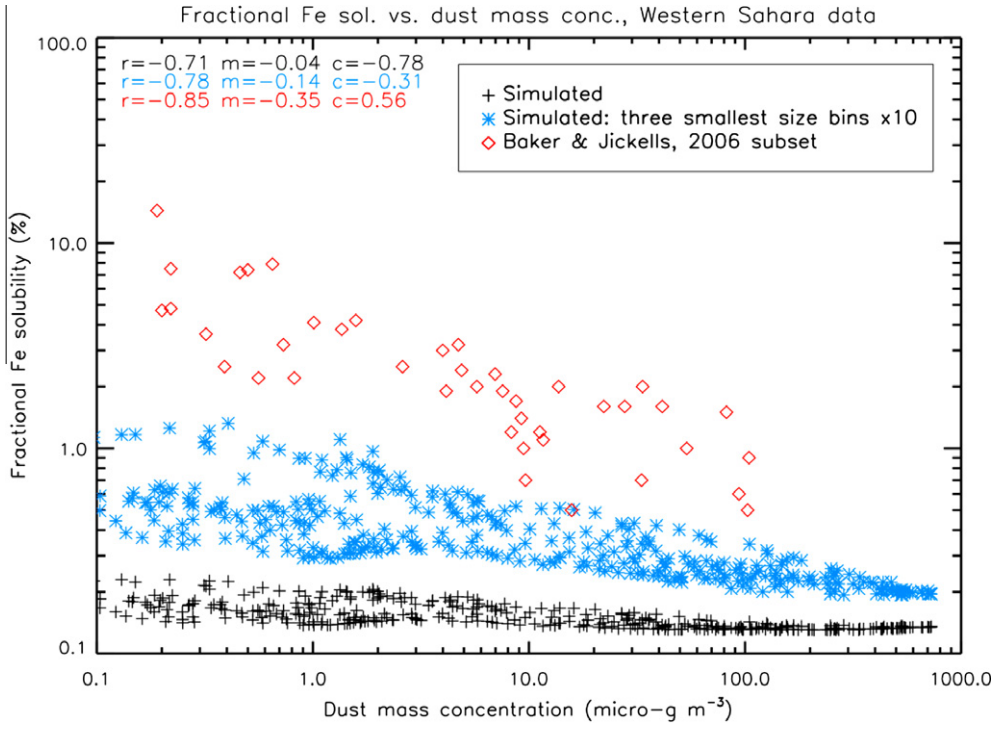

Fig. 18. Variations of FFS with dust mass concentration. Reproduced from Shi et al. (2011c) with permission of the authors.

Author's personal copy

4. Laboratory simulations of (warm) cloud processing indicated that a significant amount of Fe (e.g., >0.5%) can only be solubilized when the pH is lower than 4. Laboratory simulations of dust atmospheric processing showed that the FFS increases at low pH, e.g., 2, but decreases once the pH is raised to 5 or more. This has been confirmed to be due to the precipitation of Fe nanoparticles. These results suggest that unless assisted by photo-reduction and/or organic complexation, (warm) cloud processing of dust alone is unlikely to cause a large increase in the FFS. Ice cloud processing might cause the Fe to be released under photo-radiation in dust, but further work is needed to confirm this hypothesis.
5. A more recent laboratory and modelling study showed that physical size sorting alone is not the dominant mechanism causing the enhancement of the FFS in dust aerosol particles during transport. This suggests that future studies to model the dust FFS should focus on dust chemical processing and/or dust mixing with anthropogenic particles.
6. Photo-reduction and organic complexation appear to be less important in mobilizing insoluble Fe in cloud conditions for dust aerosol particles. But photoreduction is pH and organic matter dependent, and pH also depends on solid/liquid ratios. Thus, it is not straightforward to simply separate out these effects. Furthermore, organic matter may keep Fe in a bioavailable and organically complexed form after being acid solubilized so again these factors are not easily separated. More work on the nature of the organic matter in the atmospheric aerosols and cloud water and their complexing reaction constants are needed. Laboratory work to quantify the rates of reaction of photo-radiation during atmospherically relevant acid and cloud processing are also necessary. Detailed study of rainwater will provide useful insights in understanding the Fe solubilization and complexation processes in atmospheric water.

Acknowledgements

We thank Natural Environment Research Council Fellowship (NE/I021616/1: Z. Shi) and QUEST-Dust (K. Carslaw) for funding. The principal author started to write this manuscript while he was hosted at SEE of the University of Leeds (partly funded by QUEST-Dust and Prof. M. Krom). A major part of the manuscript was completed at the University of Birmingham. We deeply thank the two reviewers for their detailed and constructive comments. Thanks are also paid to Prof. Zhang and Dr. Ogata from Prefectural University of Kumamoto, Japan, Dr. Mackie from University of Otago, and Dr. Buck from University of California, Santa Cruz for providing original data for some of the figures.

References

Achilles, K.M. et al., 2003. Bioavailability of iron to Trichodesmium colonies in the western subtropical Atlantic Ocean. Limnol. Oceanogr. 48, 2250–2255.

Aguilar-Islas, A.M., Wu, J., Rember, R., Johansen, A.M., Shank, L.M., 2010. Dissolution of aerosol-derived iron in seawater: leach solution chemistry, aerosol type, and colloidal iron fraction. Mar. Chem. 120, 25–33.

Arimoto, R., Balsam, W., Schloesslin, C., 2002. Visible spectroscopy of aerosol particles collected on filters: iron-oxide minerals. Atmos. Environ. 36, 89–96.

Arimoto, R., Kim, Y.J., Kim, Y.P., Quinn, P.K., Bates, T.S., Anderson, T.L., Gong, S., Uno, I., Chin, M., Huebert, B.J., Clarke, A.D., Shinozuka, Y., Weber, R.J., Anderson, J.R., Guazzotti, S.A., Sullivan, R.C., Sodeman, D.A., Prather, K.A., Sokolik, I.N., 2006. Characterization of Asian Dust during ACE-Asia. Monitoring and modelling of Asian dust storms. Global Planet. Change 52, 23–56.

Arnold, E., Merrill, J., Leinen, M., King, J., 1998. The effect of source area and atmospheric transport on mineral aerosol collected over the North Pacific Ocean. Global Planet. Change 18, 137–159.

Avila, A., Queralt-Mitjans, I., Alarcon, M., 1997. Mineralogical composition of African dust delivered by red rains over northeastern Spain. J. Geophys. Res. 102, 21977–21996.

Azuma, K., Kametani, H., 1964. Kinetics of dissolution of ferric oxide. Trans. Metall. Soc. AIME 230, 853–862.

Baker, A.R., Kelly, S.D., Biswas, K.F., Witt, M., Jickells, T.D., 2003. Atmospheric deposition of nutrients to the Atlantic Ocean. Geophys. Res. Lett. 30, 2296. http://dx.doi.org/10.1029/2003GL018518.

Baker, A.R., Croot, P.L., 2010. Atmospheric and marine controls on aerosol iron solubility in seawater. Mar. Chem. 120, 4–13.

Baker, A.R., French, M., Linge, K.L., 2006a. Trends in aerosol nutrient solubility along a west–east transect of the Saharan dust plume. Geophys. Res. Lett. 33, L07805. http://dx.doi.org/10.1029/2005GL024764.

Baker, A.R., Jickells, T.D., Witt, M., Linge, K.L., 2006b. Trends in the solubility of iron, aluminium, manganese and phosphorus in aerosol collected over the Atlantic Ocean. Mar. Chem. 98, 43–58.

Baker, A.R., Jickells, T.D., 2006. Mineral particle size as a control on aerosol iron solubility. Geophys. Res. Lett. 33, L17608. http://dx.doi.org/10.1029/2006GL026557.

Baker, A.R., Weston, K., Kelly, S.D., Voss, M., Streu, P., Cape, J.N., 2007. Dry and wet deposition of nutrients from the tropical Atlantic atmosphere: links to primary productivity and nitrogen fixation. Deep-Sea Res. Part I 54, 1704–1720.

Bergametti, G., Gomes, L., Coude-Gaussen, G., Rognon, P., Le Costumer, M., 1989. African dust over Canary Islands: source regions, identification and transport pattern for some summer situations. J. Geophys. Res. 94, 14855–14864.

Bonnet, S., Guieu, C., 2004. Dissolution of atmospheric iron in seawater. Geophys. Res. Lett. 31, L03303. http://dx.doi.org/10.1029/2003GL018423.

Bonneville, S., Behrends, T., Van Cappellen, P., 2009. Solubility and dissimilatory reduction kinetics of iron(III) oxyhydroxides: a linear free energy relationship. Geochim. Cosmochim. Acta 73, 5273–5282.

Boyd, P.W., McTainsh, G., Sherlock, V., Richardson, K., Nichol, S., Ellwood, M., Frew, R., 2004. Episodic enhancement of phytoplankton stocks in New Zealand subantarctic waters: Contribution of atmospheric and oceanic iron supply. Global Biogeochem. Cycles 18, GB1029. http://dx.doi.org/10.1029/2002GB002020.

Boyd, P., Jickells, T.D., Law, C.S., Blain, S., Boyle, E.A., Buesseler, K.O., Coale, K.H., Cullen, J.J., de Baar, H.J.W., Follows, M., Harvey, M., Lancelot, C., Levasseu, M., Owens, N.P.J., Pollard, R., Rivkin, R.B., Sarmiento, J., Schoemann, V., Smetacek, V., Takeda, S., Tsuda, A., Turner, S., Watson, A.J., 2007. Mesoscale iron enrichment experiments 1993–2005: synthesis and future directions. Science 315, 612–617.

Breitbarth, E., Achterberg, E.P., Ardelan, M.V., Baker, A.R., Bucciarelli, E., Chever, F., Croot, P.L., Duggen, S., Gledhill, M., Hassellov, M., Hassler, C., Hoffmann, L.J., Hunter, K.A., Hutchins, D.A., Ingri, J., Jickells, T., Lohan, M.C., Nielsdottir, M.C., Sarthou, G., Schoemann, V., Trapp, J.M., Turner, D.R., Ye, Y., 2010. Iron biogeochemistry across marine systems-progress from the past decade. Biogeoscience 7, 1075–1097.

Bristow, C.S., Hudson-Edwards, K.A., Chappell, A., 2010. Fertilizing the Amazon and equatorial Atlantic with West African dust. Geophys. Res. Lett. 37, L14807. http://dx.doi.org/10.1029/2010GL043486.

Buck, C.S., Landing, W.M., Resing, J.A., Lebon, G.T., 2006. Aerosol iron and aluminum solubility in the northwest Pacific Ocean: results from the 2002 IOC cruise. Geochem. Geophys. Geosyst. 7, Q04M07. http://dx.doi.org/10.1029/2005GC000977.

Buck, C.S., Landing, W.M., Resing, J.A., Measures, C.I., 2010a. The solubility and deposition of aerosol Fe and other trace elements in the North Atlantic Ocean: observations from the A16N CLIVAR/CO2 repeat hydrography section. Mar. Chem. 120, 57–70.

Buck, C.S., Landing, W.M., Resing, J.A., 2010b. Particle size and aerosol iron solubility: a high resolution analysis of Atlantic aerosols. Mar. Chem. 120, 14–24.

Buseck, P.R., Posfai, M., 1999. Airborne minerals and related aerosol particles: effects on climate and the environment. Proc. Natl. Acad. Sci. USA 96, 3372–3379.

Chen, Y., Paytan, A., Chase, Z., Measures, C., Beck, A.J., Sanudo-Wilhelmy, S.A., Post, A.F., 2008. Sources and fluxes of atmospheric trace elements to the Gulf of Aqaba, Red Sea. J. Geophys. Res. 113, D05306. http://dx.doi.org/10.1029/2007JD009110.

Chen, Y., Siefert, R.L., 2003. Determination of various types of labile atmospheric iron over remote oceans. J. Geophys. Res. 108 (D24), 4774. http://dx.doi.org/10.1029/2003JD003515.

Chen, Y., Siefert, R.L., 2004. Seasonal and spatial distributions and dry deposition fluxes of atmospheric total and labile iron over the tropical and subtropical North Atlantic Ocean. J. Geophys. Res. 109, D09305. http://dx.doi.org/10.1029/2003JD003958.

Chen, Y., Street, J., Paytan, A., 2006. Comparison between pure-water- and seawater-soluble nutrient concentrations of aerosols from the Gulf of Aqaba. Mar. Chem. 101, 141–152.

Chester, R., Baxter, G.G., Behairy, A.K.A., Connor, K., Cross, D., Elderfield, H., Padgham, R.C., 1977. Soil-sized eolian dusts from the lower troposphere of the eastern Mediterranean Sea. Mar. Geol. 24, 201–217.

Chou, C., Formenti, P., Maille, M., Ausset, P., Helas, G., Harrison, M., Osborne, S., 2008. Size distribution, shape, and composition of mineral dust aerosols collected during the African Monsoon Multidisciplinary Analysis Special Observation Period: Dust and Biomass-Burning Experiment field campaign in Niger, January 2006. J. Geophys. Res. 113, D00C10. http://dx.doi.org/10.1029/2008JD009897.

Chuang, P.Y., Duvall, R.M., Shafer, M.M., Schauer, J.J., 2005. The origin of water soluble particulate iron in the Asian atmospheric outflow. Geophys. Res. Lett. 32 (7), L07813.

Author's personal copy

Clarke, A.D., Shinozuka, Y., Kapustin, V.N., Howell, S., Huebert, B., Doherty, S., Anderson, T., Covert, D., Anderson, J., Hua, X., Moore II, K.G., McNaughton, C., Carmichael, G., Weber, R., 2004. Size distributions and mixtures of dust and black carbon aerosol in Asian outflow: physiochemistry and optical properties. J. Geophys. Res. 109, D15S09. http://dx.doi.org/10.1029/2003JD004378.

Collett Jr., J.L., Bator, A., Rao, X., Demoz, B.B., 1994. Acidity variations across the cloud drop size spectrum and their influence on rates of atmospheric sulfate production. Geophys. Res. Lett. 21 (22), 2393–2396. http://dx.doi.org/10.1029/94GL02480.

Cornell, R.M., Schwertmann, U., 2003. The Iron Oxides: Structure, Properties, Reactions, Occurrence and Uses. Wiley-VCH Publishers, New York.

Coz, E., Gomez-Moreno, F.J., Pujadas, M., Casuccio, G.S., Lersch, T.L., Artinano, B., 2009. Individual particle characteristics of North African dust under different long-range transport scenarios. Atmos. Environ. 43, 1850–1863.

Croot, P.L., Hunter, K.A., 1998. Trace metal distributions across the continental shelf near Otago Peninsula, New Zealand. Mar. Chem. 62, 185–201.

Cwiertny, D.M., Baltrusaitis, J., Hunter, G.J., Laskin, A., Scherer, M.M., Grassian, V.H., 2008a. Characterization and acid-mobilization study of iron-containing mineral dust source materials. J. Geophys. Res. 113, D05202. http://dx.doi.org/10.1029/2007JD009332.

Cwiertny, D.M. et al., 2008b. Surface chemistry and dissolution of α-FeOOH nanorods and microrods: environmental implications of size-dependent interactions with oxalate. J. Phys. Chem. C 113 (6), 2175.

Dall'Osto, M., Harrison, R.M., Highwood, E.J., O'Dowd, C., Ceburnis, D., Querol, X., Achterberg, E.P., 2010. Variation of the mixing state of Saharan dust particles with atmospheric transport. Atmos. Environ. 44, 3135–3146. http://dx.doi.org/10.1016/j.atmosenv.2010.05.030.

de Baar, H.J.W. et al., 2005. Synthesis of 8 iron fertilization experiments: from the iron age to the age of enlightenment. J. Geophys. Res. 110, C09S16. http://dx.doi.org/10.1029/2004JC002601.

Deguillaume, L., Leriche, M., Desboeufs, K., Mailhot, G., George, C., Chaumerliac, N., 2005. Transition metals in atmospheric liquid phases: sources, reactivity, and sensitive parameters. Chem. Rev. 105 (9), 3388–3431.

Deguillaume, L., Desboeufs, K.V., Leriche, M., Long, Y., Chaumerliac, N., 2010. Effect of iron dissolution on cloud chemistry: from laboratory measurements to model results. Atmos. Pollut. Res. 1 (4), 220–228. http://dx.doi.org/10.5094/APR.2010.029, 2010.

DeMott, P.J., Sassen, K., Poellot, M.R., Baumgardner, D., Rogers, D.C., Brooks, S.D., Prenni, A.J., Kreidenweis, S.M., 2003. African dust aerosols as atmospheric ice nuclei. Geophys. Res. Lett. 30 (14), 1732. http://dx.doi.org/10.1029/2003GL017410.

Desboeufs, K.V., Sofikitis, A., Losno, R., Colin, J.L., Ausset, P., 2005. Dissolution and solubility of trace metals from natural and anthropogenic aerosol particulate matter. Chemosphere 58, 195–203. http://dx.doi.org/10.1016/j.chemosphere.2004.02.025.

Desboeufs, K., Losno, R., Vimeux, F., Cholbi, S., 1999. PH dependent dissolution of wind transported Saharan dust. J. Geophys. Res. 104, 21287–21299.

Desboeufs, K.V., Losno, R., Colin, J.L., 2001. Factors influencing aerosol solubility during cloud processes. Atmos. Environ. 35, 3529–3537.

Duggen, S. et al., 2007. Subduction zone volcanic ash can fertilize the surface ocean and stimulate phytoplankton growth: evidence from biogeochemical experiments and satellite data. Geophys, Res. Lett. 34, L01612.

Duggen, S. et al., 2010. The role of airborne volcanic ash for the surface ocean biogeochemical iron cycle: a review. Biogeoscience 7, 827–844.

Elrod, V.A. et al., 2004. The flux of iron from continental shelf sediments: a missing source for global budgets. Geophys. Res. Lett. 31, L12307. http://dx.doi.org/10.1029/2004GL020216.

Engelhart, G.J., Hildebrandt, L., Kostenidou, E., Mihalopoulos, N., Donahue, N.M., Pandis, S.N., 2011. Water content of aged aerosol. Atmos. Chem. Phys. 11, 911–920. http://dx.doi.org/10.5194/acp-11-911-2011.

Erel, Y., Pehkonen, S.O., Hoffmann, M.R., 1993. Redox chemistry of iron in fog and stratus Clouds. J. Geophys. Res. 98, 18423–18434.

Ervens, B., Turpin, B.J., Weber, R.J., 2011. Secondary organic aerosol formation in cloud droplets and aqeous particles (aqSOA): a review of laboratory, field and model studies. Atmos. Chem. Phys. 11, 11069–11102. http://dx.doi.org/10.5194/acp-11-11069-2011.

Falconer, R.E., Falconer, P.D., 1980. Determination of cloud water acidity at a mountain observatory in the Adirondack Mountains of New York state. J. Geophys. Res. 85 (C12), 7465–7470. http://dx.doi.org/10.1029/JC085iC12p07465.

Fan, S.-M., Moxim, W.J., Levy II, H., 2006. Aeolian input of bioavailable iron to the ocean. Geophys. Res. Lett. 33, L07602. http://dx.doi.org/10.1029/2005GL024852.

Faust, B.C., Hoigne, J., 1990. Photolysis of Fe(III)-hydroxy complexes as sources of OH radicals in clouds, fog and rain. Atmos. Environ. 24, 79–89.

Faust, B.C., Zepp, R.G., 1993. Photochemistry of aqueous iron(III)-polycarboxylate complexes: roles in the chemistry of atmospheric and surface waters. Environ. Sci. Technol. 27 (12), 2517–2522.

Fontes, M.P.F., Wee, S.B., 1996. Phosphate adsorption by clays from Brazilian oxisols: relationships with specific surface area and mineralogy. Geoderma 72, 37–51.

Formenti, P. et al., 2008. Regional variability of the composition of mineral dust from western Africa: results from the AMMA SOP0/DABEX and DODO field campaigns. J. Geophys. Res. 113, D00C13. http://dx.doi.org/10.1029/2008JD009903.

Formenti, P., Schuetz, L., Balkanski, Y., Desboeufs, K., Ebert, M., Kandler, K., Petzold, A., Scheuvens, D., Weinbruch, S., Zhang, D., 2011. Recent progress in understanding physical and chemical properties of African and Asian mineral dust. Atmos. Chem. Phys. 11, 8231–8256. http://dx.doi.org/10.5194/acp-11-8231-2011.

Fu, H., Cwiertny, D.M., Carmichael, G.R., Scherer, M.M., Grassian, V.H., 2010. Photoreductive dissolution of Fe-containing mineral dust particles in acidic media. J. Geophys. Res. 115, D11304. http://dx.doi.org/10.1029/2009JD012702.

Garvie, L.A.J., Buseck, P.R., 1998. Ratios of ferrous to ferric iron from nanometer-sized areas in minerals. Nature 396, 667–670. http://dx.doi.org/10.1038/25334.

Gioda, A., Mayol-Bracero, O.L., Morales-García, F., Collett, J., Decesari, S., Emblico, L., Facchini, M.C., Morales-De Jesús, R.J., Mertes, S., Borrmann, S., Walter, S., Schneider, J., 2009. Chemical composition of cloud water in the Puerto Rican tropical trade wind cumuli. Water Air Soil Pollut. 200, 3–14. http://dx.doi.org/10.1007/s11270-008-9888-4.

Guieu, C., Loye-Pilot, M.D., Ridame, C., Thomas, C., 2002. Chemical characterization of the Saharan dust end-member: some biogeochemical implications for the western Mediterranean Sea. J. Geophys. Res. 107 (D15), 4258. http://dx.doi.org/10.1029/2001JD00582.

Hand, J.L., Mahowald, N.M., Chen, Y., Siefert, R.L., Luo, C., Subramaniam, A., Fung, I., 2004. Estimates of atmospheric-processed soluble iron from observations and a global mineral aerosol model: biogeochemical implications. J. Geophys. Res. 109, D17205. http://dx.doi.org/10.1029/2004JD004574.

Hand, V.L., Capes, G., Vaughan, D.J., Formenti, P., Haywood, J.M., Coe, H., 2010. Evidence of internal mixing of African dust and biomass burning particles by individual particle analysis using electron beam techniques. J. Geophys. Res. 115, D13301. http://dx.doi.org/10.1029/2009JD012938.

Haywood, J.M. et al., 2008. Overview of the dust and biomass-burning experiment and african monsoon multidisciplinary analysis special observing period-0. J. Geophys. Res. 113, D00C17. http://dx.doi.org/10.1029/2008JD010077.

He, K., Zhao, Q., Ma, Y., Duan, F., Yang, F., Shi, Z., Chen, G., 2012. Spatial and seasonal variability of PM2.5 acidity at two Chinese megacities: insights into the formation of secondary inorganic aerosols. Atmos. Chem. Phys. 12 (1377–1395), 2012. http://dx.doi.org/10.5194/acp-12-1377-2012.

Hegg, D.A., Gao, S., Jonsson, H., 2002. Measurements of selected dicarboxylic acids in marine cloud water. Atmos. Res. 62, 1–10.

Heller, M.I., Croot, P.L., 2011. Superoxide decay as a probe for speciation changes during dust dissolution in Tropical Atlantic surface waters near Cape Verde. Mar. Chem. 126 (1–4), 37–55.

Hsu, S.C., Wong, G.T.F., Gong, G.C., Shiah, F.K., Huang, Y.T., Kao, S.J., Tsai, F., Lung, S.C.C., Lin, F.J., Lin, I.I., 2010. Sources, solubility, and dry deposition of aerosol trace elements over the East China Sea. Mar. Chem. 120, 116–127.

Hyacinthe, C., Bonneville, S., Van Cappellen, P., 2006. Reactive iron (III) in sediments: chemical versus microbial extractions. Geochim. Cosmochim. Acta 70, 4166–4180.

Hyacinthe, C., Van Cappellen, P., 2004. An authigenic iron phosphate phase in estuarine sediments: composition, formation and chemical reactivity. Mar. Chem. 91, 227–251.

Ito, A., Feng, Y., 2010. Role of dust alkalinity in acid mobilization of iron. Atmos. Chem. Phys. 10, 9237–9250. http://dx.doi.org/10.5194/acp-10-9237-2010.

Ito, A., 2012. Contrasting the effect of iron mobilization on soluble iron deposition to the ocean in the northern and southern hemispheres. J. Meteoro. Soc. Japan 90A, 67–188.

Jaenicke, R., Schutz, L., 1978. Comprehensive study of physical and chemical properties of the surface aerosols in the Cape Verde islands region. J. Geophys. Res. 83 (C7), 3585–3599.

Jickells, T.D., Spokes, L.J., 2001. Atmospheric iron inputs to the oceans. In: Turner, D.R., Hunter, K. (Eds.), The Biogeochemistry of Iron in Seawater. SCOR/IUPAC Series. J. Wiley, pp. 85–121.

Jickells, T.D., An, Z.S., Andersen, K.K., Baker, A.R., Bergametti, G., Brooks, N., Cao, J.J., Boyd, P.W., Duce, R.A., Hunter, K.A., Kawahata, H., Kubilay, N., LaRoche, J., Liss, P.S., Mahowald, N., Prospero, J.M., Ridgwell, A.J., Tegen, I., Torres, R., 2005. Global iron connections between desert dust, ocean biogeochemistry, and climate. Science 308, 67–71.

Johnson, M.S., Meskhidze, N., Solmon, F., Gassó, S., Chuang, P.Y., Gaiero, D.M., Yantosca, R.M., Wu, S., Wang, Y., Carouge, C., 2010. Modeling dust and soluble iron deposition to the South Atlantic Ocean. J. Geophys. Res. 115, D15202. http://dx.doi.org/10.1029/2009JD013311.

Journet, E., Desboeufs, K.V., Caquineau, S., Colin, J.-L., 2008. Mineralogy as a critical factor of dust iron solubility. Geophys. Res. Lett. 35, L07805. http://dx.doi.org/10.1029/2007GL031589.

Kandler, K. et al., 2009. Size distribution, mass concentration, chemical and mineralogical composition and derived optical parameters of the boundary layer aerosol at Tinfou, Morocco, during SAMUM 2006. Tellus B 61, 32–50.

Kandler, K., Benker, N., Bundke, U., Cuevas, E., Ebert, M., Knippertz, P., Rodriguez, S., Schutz, L., Weinbruch, S., 2007. Chemical composition and complex refractive index of Saharan mineral dust at Izana, Tenerife (Spain) derived by electron microscopy. Atmos. Environ. 41, 8058–8074.

Kandler, K., Schutz, L., Jackel, S., Lieke, K., Emmel, C., Muller-Ebert, D., Ebert, M., Scheuvens, D., Schladitz, A., Segvic, B., Wiedensohler, A., Weinbruch, S., 2011. Ground-based off-line aerosol measurements at Praia, Cape Verde, during the Saharan mineral Dust Experiment: microphysical properties and mineralogy. Tellus B 63, 475–496. http://dx.doi.org/10.1111/j.1600-0889.2011.00546.x.

Kieber, R.J. et al., 2005. Organic complexation of Fe(II) and its impact on the redox cycling of iron in rain. Environ. Sci. Technol. 39, 1576–1583.

Author's personal copy

Kim, K., Choi, W., Hoffmann, M.R., Yoon, H.I., Park, B.K., 2010. Photoreductive dissolution of iron oxides trapped in ice and its environmental implications. Environ. Sci. Technol. 44, 4142–4148.
Kostka, J.E., Luther III, G.W., 1994. Partitioning and speciation of solid phase iron in saltmarsh sediments. Geochim. Cosmochim. Acta 58, 1701–1710.
Kuma, K. et al., 1998a. Spatial variability of Fe(III) hydroxide solubility in the water column of the northern North Pacific Ocean. Deep-Sea Res. 45, 91–113.
Kuma, K. et al., 1998b. Size-fractionated iron concentrations and Fe(III) hydroxide solubilities in various coastal waters. Estuar. Coast. Shelf Sci. 47 (3), 275–283.
Kumar, A., Sarin, M.M., 2010. Aerosol iron solubility in a semi-arid region: temporal trend and impact of anthropogenic sources. Tellus B 62, 125–132. http://dx.doi.org/10.1111/j.1600-0889.2009.00448.x.
Kumar, P., Sokolik, I.N., Nenes, A., 2011. Measurements of cloud condensation nuclei activity and droplet activation kinetics of fresh unprocessed regional dust samples and minerals. Atmos. Chem. Phys. 11, 3527–3541.
Lafon, S., Rajot, J.L., Alfaro, S.C., Gaudichet, A., 2004. Quantification of iron oxides in desert aerosol. Atmos. Environ. 38, 1211–1218.
Lafon, S., Sokolik, I.N., Rajot, J.L., Caquineau, S., Gaudichet, A., 2006. Characterization of iron oxides in mineral dust aerosols: implications for light absorption. J. Geophys. Res. 111, D21207. http://dx.doi.org/10.1029/2005JD007016.
Lambert, F. et al., 2008. Dust-climate couplings over the past 800,000 years from the EPICA Dome C ice core. Nature 452, 616–619.
Lazaro, F.J., Gutierrez, L., Barron, V., Gelado, M.D., 2008. The speciation of iron in desert dust collected in Gran Canaria (Canary Islands): combined chemical, magnetic and optical analysis. Atmos. Environ. 42, 8887–8896. http://dx.doi.org/10.1016/j.atmosenv.2008.09.035.
Leigh, D.S., 1996. Soil chronosequence of Brasstown Creek, Blued Ridge Mountains, USA. Catena 26, 99–114.
Leinen, M., Prospero, J.M., Arnold, E., Blank, M., 1994. Mineralogy of aeolian dust reaching the North Pacific Ocean: 1. Sampling and analysis. J. Geophys. Res. 99, 21017–21023.
Lieke, K., Kandler, K., Scheuvens, D., Emmel, C., Von Glahn, C., Petzold, A., Weinzierl, B., Veira, A., Ebert, M., Weinbruch, S., Schutz, L., 2011. Particle chemical properties in the vertical column based on aircraft observations in the vicinity of Dpe Verde islands. Tellus B 63, 497–511. http://dx.doi.org/10.1111/j.1600-0889.2011.00553.x.
Liu, X., Millero, F.J., 1999. The solubility of iron in sodium chloride solutions. Geochim. Cosmochim. Acta 63, 3487–3497.
Liu, X., Millero, F.J., 2002. The solubility of iron in seawater. Mar. Chem. 77, 43–54. http://dx.doi.org/10.1016/S0304-4203(01)00074-3.
Luo, C., Mahowald, N.M., Meskhidze, N., Chen, Y., Siefert, R.L., Baker, A.R., Johansen, A.M., 2005. Estimation of iron solubility from observations and a global aerosol model. J. Geophys. Res. 110, D23307. http://dx.doi.org/10.1029/2005JD006059.
Luo, C., Mahowald, N., Bond, T., Chuang, P.Y., Artaxo, P., Siefert, R., Chen, Y., Schauer, J., 2008. Combustion iron distribution and deposition. Global Biogeochem. Cycles 22, GB1012. http://dx.doi.org/10.1029/2007GB002964.
Mackie, D.S., Boyd, P.W., Hunter, K.A., McTainsh, G.H., 2005. Simulating the cloud processing of iron in Australian dust: pH and dust concentration. Geophys. Res. Lett. 32, L06809. http://dx.doi.org/10.1029/2004GL022122.
Mackie, D.S., Boyd, P.W., McTainsh, G.H., Tindale, N.W., Westberry, T.K., Hunter, K.A., 2008. Biogeochemistry of iron in Australian dust: from eolian uplift to marine uptake. Geochem. Geophys. Geosyst. 9, Q03Q08. http://dx.doi.org/10.1029/2007GC001813.
Mackie, D.S., Peat, J.M., McTainsh, G.H., Boyd, P.W., Hunter, K.A., 2006. Soil abrasion and eolian dust production: Implications for iron partitioning and solubility. Geochem. Geophys. Geosyst. 7, Q12Q03. http://dx.doi.org/10.1029/2006GC001404.
Mahaffey, C., Williams, R.G., Wolff, G.A., Mahowald, N., Anderson, W., Woodward, M., 2003. Biogeochemical signatures of nitrogen fixation in the eastern North Atlantic. Geophys. Res. Lett. 30 (6), 1300. http://dx.doi.org/10.1029/2002GL016542.
Mahowald, N.M. et al., 2009. Atmospheric iron deposition: global distribution, variability, and human perturbations. Annu. Rev. Mar. Sci. 1, 245–278.
Mahowald, N.M., Baker, A.R., Bergametti, G., Brooks, N., Duce, R.A., Jickells, T.D., Kubilay, N., Prospero, J.M., Tegen, I., 2005. Atmospheric global dust cycle and iron inputs to the ocean. Global Biogeochem. Cycles 19, GB4025. http://dx.doi.org/10.1029/2004GB002402.
Majestic, B.J., Schauer, J.J., Shafer, M.M., 2007. Application of synchrotron radiation for measurement of iron red-ox speciation in atmospherically processed aerosols. Atmos. Chem. Phys. 7, 2475–2487.
Manktelow, P.T., Carslaw, K.S., Mann, G.W., Spracklen, D.V., 2010. The impact of dust on sulfate aerosol, CN and CCN during an East Asian dust storm. Atmos. Chem. Phys. 10, 365–382. http://dx.doi.org/10.5194/acp-10-365-2010.
Marinoni, A., Laj, P., Sellegri, K., Mailhot, G., 2004. Cloud chemistry at the Puy de Dôme: variability and relationships with environmental factors. Atmos. Chem. Phys. 4, 715–728.
Martin, J.H., 1990. Glacial–interglacial CO_2 change: the iron hypothesis. Paleoceanography 5, 1–13.
Martin, J.H., Fitzwater, S.E., 1988. Iron deficiency limits phytoplankton growth in the north-east Pacific subarctic. Nature 331, 341–343. http://dx.doi.org/10.1038/331341a0.
Martin, J.H., Gordon, R.M., Fitzwater, S., Broenkow, W.W., 1989. VERTEX: phytoplankton/iron studies in the Gulf of Alaska. Deep-Sea Res. 36, 649–680.
Matsuki, A., Schwarzenboeck, A., Venzac, H., Laj, P., Crumeyrolle, S., Gomes, L., 2010. Cloud processing of mineral dust: direct comparison of cloud residual and clear sky particles during AMMA aircraft campaign in summer 2006. Atmos. Chem. Phys. 10, 1057–1069.
McConnell, C.L., Highwood, E.J., Coe, H., Formenti, P., Anderson, B., Osborne, S., Nava, S., Desboeufs, K., Chen, G., Harrison, M.A.J., 2008. Seasonal variations of the physical and optical characteristics of Saharan dust: results from the Dust Outflow and Deposition to the Ocean (DODO) experiment. J. Geophys. Res. 113, D14S05. http://dx.doi.org/10.1029/2007JD009606.
McFadden, I.D., Hendricks, D.M., 1985. Changes in the content and composition of pedogenic iron oxyhydroxides in a chronosequence of soils in Southern California. Quart. Res. 23, 189–204.
McTainsh, G.H., 1989. Quaternary aeolian dust processes and sediments in the Australian region. Quat. Sci. Rev. 8 (3), 235–253.
Mehra, O.P., Jackson, M.L., 1960. Iron oxide removal from soils and clays by a dithionite-citrate buffered with sodium bicarbonate. Clay Miner. 7, 317–327.
Merrill, J., Arnold, E., Leinen, M., Weaver, C., 1994. Mineralogy of aeolian dust reaching the North Pacific Ocean: 2. Relationship of mineral assemblages to atmospheric transport patterns. J. Geophys. Res. 99, 21025–21032.
Meskhidze, N., Chameides, W.L., Nenes, A., 2005. Dust and pollution: a recipe for enhanced ocean fertilization? J. Geophys. Res. 110, D03301. http://dx.doi.org/10.1029/2004JD005082.
Meskhidze, N., Chameides, W.L., Nenes, A., Chen, G., 2003. Iron mobilization in mineral dust: can anthropogenic SO_2 emissions affect ocean productivity? Geophys. Res. Lett. 30 (21), 2085. http://dx.doi.org/10.1029/2003GL018035.
Meunier, A., Velde, B.D., 2004. Illite: Origins, Evolution, and Metamorphism. Springer, Berlin, London.
Mills, M.M., Ridame, C., Davey, M., La Roche, J., Geider, R.J., 2004. Iron and phosphorus co-limit nitrogen fixation in the eastern tropical north Atlantic. Nature 429, 292–294.
Moore, C.M., Mills, M.M., Achterberg, E.P., Geider, R.J., LaRoche, J., Lucas, M.I., McDonagh, E.L., Pan, X., Poulton, A.J., Rijkenberg, M.J.A., Suggett, D.J., Ussher, S.J., Woodward, E.M.S., 2009. Large-scale distribution of Atlantic nitrogen fixation controlled by iron availability. Nat. Geosci. 2, 867–871. http://dx.doi.org/10.1038/ngeo667.
Moxim, W.J., Fan, S.-M., Levy II, H., 2011. The meteorological nature of variable soluble iron transport and deposition within the North Atlantic Ocean basin. J. Geophys. Res. 116, D03203. http://dx.doi.org/10.1029/2010JD014709.
Muller, C.L., Baker, A., Hutchinson, R., Fairchild, I.J., Kidd, C., 2008. Analysis of rainwater dissolved organic carbon compounds using fluorescence spectrophotometry. Atmos. Environ. 42, 8036–8045.
Muller, C.L., Kidd, C., Fairchild, I.J., Baker, A., 2010. Investigation into clouds and precipitation over an urban area using mico rain radars, satellite remote sensing and fluorescence spectrophotometry. Atmos. Res. 96, 241–255.
Nenes, A., Krom, M., Mihalopoulos, N., Van Cappellen, P., Shi, Z., Bougiatioti, A., Zarmpas, P., Herubt, B., 2011. Atmospheric acidification of mineral aerosols: a source of bioavailable phosphorus for the oceans. Atmos. Chem. Phys. 11, 6265–6272. http://dx.doi.org/10.5194/acp-11-6265-2011.
Nodwell, L.M., Price, N.M., 2001. Direct use of inorganic colloidal iron by marine mixotrophic phytoplankton. Limnol. Oceanog. 46, 765–777.
Nishioka, J., Takeda, S., de Baar, H.J.W., Croot, P.L., Boye, M., Laan, P., Timmermans, K.R., 2005. Changes in the concentration of iron in different size fractions during an iron enrichment experiment in the open Southern Ocean. Mar. Chem. 95, 51–63. http://dx.doi.org/10.1016/j.marchem.2004.06.040.
Ogata, H., Zhang, D., Yamada, M., Tobo, Y., 2011. Comparison of elemental composition of Asian dust particles at Amami and Amakusa during a dust event. J. Japan Soc. Atmos. Environ. 46, 10–19.
Ohta, A., Tsuno, H., Kagi, H., Kanai, Y., Nomura, M., Zhang, R., Terashima, N., Imai, N., 2006. Chemical compositions and XANES speciations of Fe, Mn and Zn from aerosols collected in China and Japan during dust events. Geochem. J. 40, 363–376.
Ooki, A., Nishioka, J., Ono, T., Noriki, S., 2009. Size dependence of iron solubility of Asian mineral dust particles. J. Geophys. Res. 114, D03202. http://dx.doi.org/10.1029/2008JD010804.
Ozsoy, T., Orneketkin, S., 2009. Trace elements in urban and suburban rainfall, Mersin, Northeastern Mediterranean. Atmos. Res. 94, 203–219. http://dx.doi.org/10.1016/j.atmosres.2009.05.017.
Paris, R., Desboeufs, K.V., Formenti, P., Nava, S., Chou, C., 2010. Chemical characterisation of iron in dust and biomass burning aerosols during AMMA-SOP0/DABEX: implication for iron solubility. Atmos. Chem. Phys. 10, 4273–4282. http://dx.doi.org/10.5194/acp-10-4273-2010.
Paris, R., Desboeufs, K.V., Journet, E., 2011. Variability of dust iron solubility in atmospheric waters: investigation of the role of oxalate organic complexation. Atmos. Environ. 45, 5510–5517.
Parker, A., 1970. An index of weathering for silicate rocks. Geol. Mag. 107, 501–504. http://dx.doi.org/10.1017/S0016756800058581.
Pehkonen, S.O., Siefert, R., Erel, Y., Webb, S., Hoffmann, M.R., 1993. Photoreduction of iron oxyhydroxides in the presence of important atmospheric organic compounds. Environ. Sci. Technol. 27, 2056–2062.
Petit, J.R. et al., 1999. Climate and atmospheric history of the past 420,000 years from the Vostok ice core, Antarctica. Nature 399, 429–436.
Pikridas, M., Bougiatioti, K., Engelhart, G.J., Hildebrandt, L., Kostenidou, E., Mohr, C., Kouvarakis, G., Zarmpas, P., Psichoudaki, M., Gagne, S., Mihalopoulos, N., Pilinis, C., Hillamo, R., Baltensperger, U., Kulmala, M., Pandis, S.N., 2010. The Finokalia aerosol measurement experiments – 2008 (FAME-08): an overview. Atmos. Chem. Phys. 10, 6793–6806. http://dx.doi.org/10.5194/acp-10-6793-2010.
Posfai, M., Buseck, P.R., 2010. Nature and climate effects of individual tropospheric aerosol particles. Ann. Rev. Earth Planet. Sci. 38, 17–43.

Author's personal copy

Poulton, S.W., Raiswell, R., 2002. The low-temperature geochemical cycle of iron: from continental fluxes to marine sediment deposition. Am. J. Sci. 302 (9), 774–805.

Raiswell, R., Canfield, D.E., 2012. The iron biogeochemical cycle past and present. Geochem. Perspect. 1, 1–220.

Raiswell, R., Benning, L.G., Tranter, M., Tulaczyk, S., 2008. Bioavailable iron in the Southern Ocean: the significance of the iceberg conveyor belt. Geochem. Trans. 9, 7.

Raiswell, R., Canfield, D.E., Berner, R.A., 1994. A comparison of iron extraction methods for the determination of degree of pyritization and recognition of iron-limited pyrite formation. Chem. Geo. 111, 101–111.

Raiswell, R., Vu, H.P., Brinza, L., Benning, L.G., 2010. The determination of labile Fe in ferrihydrite by ascorbic acid extraction: methodology, dissolution kinetics and loss of solubility with age and de-watering. Chem. Geo. 278, 20–79. http://dx.doi.org/10.1016/j.chemgeo.2010.09.002.

Redmond, H.E., Dial, K.D., Thompson, J.E., 2010. Light scattering and absorption by wind-blown dust: theory, measurement, and recent data. Aeolian Res. 2, 5–26.

Reid, E.A., Reid, J.S., Meier, M.M., Dunlap, M.R., Cliff, S.S., Broumas, A., Perry, K., Maring, H., 2003. Characterization of African dust transported to Puerto Rico by individual particle and size segregated bulk analysis. J. Geophys. Res. 108 (D19), 8591. http://dx.doi.org/10.1029/2002JD002935.

Reyes, I., Torrent, J., 1997. Citrate-ascorbate as a highly selective extractant for poorly crystalline iron oxides. Soil Sci. Soc. Am. J. 61, 1647–1654.

Ridgwell, A.J., Watson, A.J., 2002. Feedback between aeolian dust, climate and atmospheric CO_2 in glacial time. Paleoceanography 17, 1059.

Rosenfeld, D., Rudich, Y., Lahav, R., 2001. Desert dust suppressing precipitation: a possible desertification feedback loop. Proc. Natl. Acad. Sci. USA 98 (11), 5975–5980.

Röthlisberger, R., Bigler, M., Wolff, E.W., Joos, F., Monnin, E., Hutterli, M.A., 2004. Ice core evidence for the extent of past atmospheric CO_2 change due to iron fertilisation. Geophys. Res. Lett. 31, L16207. http://dx.doi.org/10.1029/2004GL020338.

Rubasinghege, G., Lentz, R.W., Scherer, M.M., Grassian, V.H., 2010. Simulated atmospheric processing of iron oxyhydroxide minerals at low pH: roles of particle size and acid anion in iron dissolution. Proc. Natl. Acad. Sci. USA 107, 6628–6633.

Rubin, M. et al., 2011. Dust- and mineral-iron utilization by the marine dinitrogen-fixer Trichodesmium. Nat. Geosci. 4 (8), 529–534.

Sarthou, G. et al., 2003. Atmospheric iron deposition and sea-surface dissolved iron concentrations in the eastern Atlantic Ocean. Deep-Sea Res. Part I 50, 1339–1352. http://dx.doi.org/10.1016/S0967-0637(03)00126-2.

Scheuvens, D., Kandler, K., Kupper, M., Lieke, K., Zorn, S.R., Ebert, M., Schutz, L., Weinbruch, S., 2011. Individual-particle analysis of airborne dust samples collected over Morocoo in 2006 during SAMUM 1. Tellus B 63, 512–530. http://dx.doi.org/10.1111/j.1600-0889.2011.00554.x.

Schlosser, C., Croot, P., 2009. Controls on seawater Fe(III) solubility in the Mauritanian upwelling zone. Geophys. Res. Lett. 36, L18606.

Schlosser, C., Croot, P.L., 2008. Application of cross-flow filtration for determining the solubility of iron species in open ocean seawater. Limnol. Oceanogr. Methods 6, 630–642.

Schroth, A.W., Crusius, J., Sholkovitz, E.R., Bostick, B.C., 2009. Iron solubility driven by speciation in dust sources to the ocean. Nat. Geosci. 2, 337–340.

Sedlak, D.L., Hoigné, J., David, M.M., Colvile, R.N., Seyffer, E., Acker, K., Wiepercht, W., Lind, J.A., Fuzzi, S., 1997. The cloudwater chemistry of iron and copper at Great Dun Fell, UK. Atmos. Environ. 31, 2515–2526.

Sedwick, P.N., Sholkovitz, E.R., Church, T.M., 2007. Impact of anthropogenic combustion emissions on the fractional solubility of aerosol iron: evidence from the Sargasso Sea. Geochem. Geophys. Geosyst. 8, Q10Q06. http://dx.doi.org/10.1029/2007GC001586.

Seinfeld, J.H., Pandis, S.N., 2006. Atmospheric Chemistry and Physics: From Air Pollution to Climate Change. John Wiley & Sons Inc., New York.

Shao, L.Y., Li, W.J., Yang, S.S., Shi, Z.B., Lu, S.L., 2007. Mineralogical characteristics of airborne particles collected in Beijing during severe Asian dust period in spring 2002. Sci. China D 50 (6), 953–959. http://dx.doi.org/10.1007/s11430-007-0035-7.

Shao, L., Li, W., Xiao, Z., Sun, Z., 2008. The mineralogy and possible sources of spring dust particles over Beijing. Adv. Atmos. Sci. 25, 395–403.

Shao, Y., Wyrwoll, K.H., Chappell, A., Huang, J., Lin, Z., McTainsh, G.H., Mikami, M., Tanaka, T.Y., Wang, X., Yoon, S., 2011. Dust cycle: an emerging core theme in Earth System Science. Aeolian Res. 2, 181–204.

Shen, Z.X., Cao, J.J., Zhang, X.Y., Arimoto, R., Ji, J.F., Balsam, W.L., Wang, Y.Q., Zhang, R.J., Li, X.X., 2006a. Spectroscopic analysis of iron-oxide minerals in aerosol particles from northern China. Sci. Total Environ. 367, 899–907.

Shen, Z.X., Cao, J., Li, X., Okuda, T., Wang, Y., Zhang, X., 2006b. Mass concentration and mineralogical characteristics of aerosol particles collected at Dunhuang during ACE-Asia. Adv. Atmos. Sci. 23, 291–298.

Shi, Z., Shao, L., Jones, T.P., Lu, S., 2005. Microscopy and mineralogy of airborne particles collected during severe dust storm episodes in Beijing, China. J. Geophys. Res. 110, D01303. http://dx.doi.org/10.1029/2004JD005073.

Shi, Z., Zhang, D., Hayashi, M., Ogata, H., Ji, H., Fujiie, W., 2008. Influences of sulfate and nitrate on the hygroscopic behaviour of coarse dust particles. Atmos. Environ. 42, 822–827. http://dx.doi.org/10.1016/j.atmosenv.2007.10.037.

Shi, Z., Shao, L., Jones, T.P., Whittaker, A.G., Lu, S., Berube, K.A., He, T., Richards, R.J., 2003. Characterization of airborne individual particles collected in an urban area, a satellite city and a clean air site in Beijing, 2001. Atmos. Environ. 37, 4097–4108.

Shi, Z., Krom, M.D., Bonneville, S., Baker, A.R., Jickells, T.D., Benning, L.G., 2009. Formation of iron nanoparticles and increase in iron reactivity in the mineral dust during simulated cloud processing. Environ. Sci. Technol. 43, 6592–6596. http://dx.doi.org/10.1021/es901294g.

Shi, Z., Bonneville, S., Krom, M., Carslaw, K., Jickells, T., Baker, A., Benning, L., 2011a. Dissolution kinetics of iron in the mineral dust at low pH during simulated atmospheric processing. Atmos. Chem. Phys. 11, 995–1007. http://dx.doi.org/10.5194/acp-11-995-2011.

Shi, Z., Krom, M.D., Bonneville, S., Baker, A.R., Bristow, C., Drake, N., Mann, G., Carslaw, K., McQuaid, J.B., Jickells, T., Benning, L.G., 2011b. Influence of chemical weathering and aging of iron oxides on the potential iron solubility of Saharan dust during simulated atmospheric processing. Global Biogeochem. Cycles 25, GB2010. http://dx.doi.org/10.1029/2010GB003837.

Shi, Z., Woodhouse, M., Carslaw, K., Krom, M., Baker, A., Savov, I., Mann, G., Fones, G., Brooks, B., Jickells, T., Benning, L., 2011c. Minor effect of physical size sorting on iron solubility of transported mineral dust. Atmos. Chem. Phys. 11, 8459–8469. http://dx.doi.org/10.5194/acp-11-8459-201.

Sholkovitz, E.R., Sedwick, P.N., Church, T.M., 2009. Influence of anthropogenic combustion emissions on the deposition of soluble aerosol iron to the ocean: empirical estimates for island sites in the North Atlantic. Geochim. Cosmochim. Acta 73, 3981–4003.

Siefert, R.L., Pehkonen, S.O., Erel, Y., Hoffmann, M.R., 1994. Iron photochemistry of aqueous suspensions of ambient aerosol with added organic acids. Geochim. Cosmochim. Acta 58, 3271–3279.

Sigman, D.M., Boyle, E.A., 2000. Glacial/interglacial variations in atmospheric carbon dioxide. Nature 407, 859–869.

Solmon, F., Chuang, P.Y., Meskhidze, N., Chen, Y., 2009. Acidic processing of mineral dust iron by anthropogenic compounds over the north Pacific Ocean. J. Geophys. Res. 114, D02305. http://dx.doi.org/10.1029/2008JD010417.

Spokes, J.L., Jickells, T.D., Lim, B., 1994. Solubilisation of aerosol trace metals by cloud processing: a laboratory study. Geochim. Cosmochim. Acta 58, 3281–3287.

Spokes, L.J., Jickells, T.D., 1996. Factors controlling the solubility of aerosol trace metals in the atmosphere and on mixing into seawater. Aqua. Geochem. 1, 355–374.

Stolpe, B., Guo, L., Shiller, A.M., Hassellöv, M., 2010. Size and composition of colloidal organic matter and trace elements in the Mississippi River, Pearl River and the northern Gulf of Mexico, as characterized by flow field-flow fractionation. Mar. Chem. 118, 119–128.

Straub, D.J., Lee, T., Collett Jr., J.L., 2007. Chemical composition of marine stratocumulus clouds over the eastern Pacific Ocean. J. Geophys. Res. 112, D04307. http://dx.doi.org/10.1029/2006JD007439.

Sullivan, R.C., Guazzotti, S.A., Sodeman, D.A., Prather, K.A., 2007. Direct observations 30 of the atmospheric processing of Asian mineral dust. Atmos. Chem. Phys. 7, 1213–1236. http://dx.doi.org/10.5194/acp-7-1213-2007.

Sullivan, R.C., Prather, K.A., 2007. Investigations of the diurnal cycle and mixing state of oxalic acid in individual particles in Asian aerosol outflow. Environ. Sci. Technol. 41 (23), 8062–8069.

Takahashi, Y., Higashi, M., Furukawa, T., Mitsunobu, S., 2011. Change of iron species and iron solubility in Asian dust during the long-range transport from western China to Japan. Atmos. Chem. Phys. 11, 11237–11352. http://dx.doi.org/10.5194/acp-11-11237-2011.

Theodosi, C., Markaki, Z., Mihalopoulos, N., 2010. Iron speciation, solubility, and temporal variability in wet and dry deposition in the Eastern Mediterranean. Mar. Chem. 120, 100–107.

Torrent, J., Liu, Q., Bloemendal, J., Barron, V., 2007. Magnetic enhancement and iron oxides in the upper Luochuan loess-Paleosol sequence, Chinese Loess plateau. Soil Sci. Sco. Am. J. 71, 1570–1578.

Trapp, J.M., Millero, F.J., Prospero, J.M., 2010. Trends in the solubility of iron in dust dominated aerosols in the equatorial Atlantic trade winds: importance of iron speciation and sources. Geochem. Geophys. Geosyst. 11, Q03014. http://dx.doi.org/10.1029/2009GC002651.

Upadhyay, N., Majestic, B.J., Herckes, P., 2011. Solubility and speciation of atmospheric iron in buffer systems simulating cloud conditions. Atmos. Environ. 45, 1858–1866. http://dx.doi.org/10.1016/j.atmosenv.2011.01.010.

Visser, F. et al., 2003. The role of the reactivity and content of iron of aerosol dust on growth rates of two Antarctic diatom species. J. Phycol. 39 (6), 1085–1094.

Wagener, T., Guieu, C., Losno, R., Bonnet, S., Mahowald, N., 2008a. Revisiting atmospheric dust export to the Southern Hemisphere ocean: biogeochemical implications. Global Biogeochem. Cycles 22, GB2006. http://dx.doi.org/10.1029/2007GB002984.

Wagener, T., Pulido-Villena, E., Guieu, C., 2008b. Dust iron dissolution in seawater: results from a one-year timeseries in the Mediterranean Sea. Geophys. Res. Lett. 35, L16601. http://dx.doi.org/10.1029/2008GL034581.

Wagener, T., Guieu, C., Leblond, N., 2010. Effects of dust deposition on iron cycle in the surface Mediterranean Sea: results from a mesocosm seeding experiment. Biogeosci. 7, 2769–3781. http://dx.doi.org/10.5194/bg-7-3769-2010.

Wang, Z. et al., 2009. Photochemical cycling of iron mediated by dicarboxylates: special effect of malonate. Environ. Sci. Technol. 44, 263–268.

Washington, R. et al., 2009. Dust as a tipping element: the Bodele depression. Chad. Proc. Natl. Acad. Sci. USA 106 (49), 20564–20571.

Watson, A.J., Bakker, D.C.E., Ridgwell, A.J., Boyd, P.W., Law, C.S., 2000. Effect of iron supply on Southern Ocean CO_2 uptake and implications for glacial atmospheric CO_2. Nature 407, 730–733.

Willey, J.D. et al., 2000. Temporal variability of iron speciation in coastal rainwater. J. Atmos. Chem. 37, 185–205.

Author's personal copy

Willey, J.D. et al., 2004. Effects of rainwater iron and hydrogen peroxide on iron speciation and phytoplankton growth in seawater near Bermuda. J. Atmos. Chem. 47, 209–222.
Willey, J.D. et al., 2008. Rainwater as a source of Fe(II)-stabilizing ligands to seawater. Limnol. Oceanogr. 53 (4), 1678–1684.
Willey, J. et al., 2009. Fe(II) in coastal rainwater: changing stability and concentrations. Aquat. Sci. 71, 144–150.
Wu, J., Rember, R., Cahill, C., 2007. Dissolution of aerosol iron in the surfacewaters of the North Pacific and North Atlantic oceans as determined by a semicontinuous flow through reactor method. Global Biogeochem. Cycles 21. http://dx.doi.org/10.1029/2006GB002851.
Wurzler, S., Reisin, T.G., Levin, Z., 2000. Modification of mineral dust particles by cloud processing and subsequent effects on drop size distributions. J. Geophys. Res. 105 (D4), 4501–4512. http://dx.doi.org/10.1029/1999JD900980.
Xu, N., Gao, Y., 2008. Characterization of hematite dissolution affected by oxalate coating, kinetics and pH. Appl. Geochem. 23 (4), 783.
Zhang, D., Iwasaka, Y., 1999. Nitrate and sulfate in individual Asian dust-storm particles in Beijing, China in spring of 1995 and 1996. Atmos. Environ. 33, 3213–3223.
Zhang, D., Iwasaka, Y., Matsuki, A., Ueno, K., Matsuzaki, T., 2006. Coarse and accumulation mode particles associated with Asian dust in Southwestern Japan. Atmos. Environ. 40, 1205–1215.
Zhang, D., Iwasaka, Y., Shi, G., Zang, J., Matsuki, A., Trochkine, D., 2003. Mixture state and size of Asian dust particles collected at Southwestern Japan in spring 2000. J. Geophys. Res. 108, 4760. http://dx.doi.org/10.1029/2003jd003869.
Zhang, Q., Jimenez, J.L., Worsnop, D.R., Canagaratna, M., 2007. A case study of urban particle acidity and its influence on secondary organic aerosol. Environ. Sci. Technol. 41, 3213–3219. http://dx.doi.org/10.1021/es061812j.
Zhu, X.R., Prospero, J.M., Millero, F.J., Savoie, D.L., 1993. The photochemical reaction in marine aerosol solution and its impact to iron concentration. J. Geophys. Res. 98, 9039–9047.
Zhu, X., Prospero, J.M., Millero, F.J., Savoie, D.L., Brass, G.W., 1992. The solubility of ferric ion in marine mineral aerosol solutions at ambient relative humidities. Mar. Chem. 38, 91–107.
Zhuang, G., Duce, R., 1993. The adsorption of dissolved iron on marine aerosol particles in surface waters of the open ocean. Deep-Sea Res. 40, 1413–1429.
Zinder, B., Furrer, G., Stumm, W., 1986. The coordination chemistry of weathering: II. Dissolution of Fe(III) oxides. Geochim. Cosmochim. Acta 50, 1861–1869.